Master's Thesis
Meteorology

EXTRATROPICAL TRANSITION AND CHARACTERISTICS OF STORM MAURI IN SEPTEMBER 1982

Terhi Laurila
(11.4.2016)

Supervisors: Dr. Hilppa Gregow and Dr. Victoria Sinclair
Examiners: Dr. Hilppa Gregow and Prof. Heikki Järvinen

UNIVERSITY OF HELSINKI
DEPARTMENT OF PHYSICS

PL 64 (Gustaf Hällströmin katu 2)
00 014 Helsingin yliopisto

HELSINGIN YLIOPISTO
HELSINGFORS UNIVERSITET
UNIVERSITY OF HELSINKI

Tiedekunta/Osasto Fakultet/Sektion – Faculty	Laitos/Institution– Department	
Faculty of Science	Department of Physics	
Tekijä/Författare – Author		
Terhi Laurila		
Työn nimi/Arbetets titel – Title		
Extratropical transition and characteristics of storm Mauri in September 1982		
Oppiaine /Läroämne – Subject		
Meteorology		
Työn laji/Arbetets art – Level	Aika/Datum – Month and year	Sivumäärä/ Sidoantal – Number of pages
Master's thesis	4/2016	51

Tiivistelmä/Referat – Abstract

An intense storm named Mauri swept over Lapland, Finland on the 22nd of September 1982 causing 3 Mm^3 forest damage and two fatalities. There were thoughts that Mauri originated from a category 4 hurricane Debby but the linkage between Debby and Mauri and their connection to climatic conditions have not been investigated before.

In this thesis, a climatic overview of September 1982 in comparison to 1981-2010 Septembers is provided. The calculations are based on ERA-Interim reanalysis data produced by European Centre for Medium-Range Weather Forecasts. The track of the storm is determined from ERA-Interim data from the time Debby occurred until Mauri crossed Finland. The evolution of Debby is also presented with the storm track data by National Oceanic and Atmospheric Administration to comparison. Extratropical transition (ET) and phase diagram of Debby and the synoptic evolution of Mauri are examined. ET is defined to start when the cyclone loses a symmetric hurricane eye feature to form asymmetric fronts, and ET is completed when the warm core of the storm turns cold. A comparison between Mauri and two other intense storms that have affected Europe is briefly presented.

It was discovered, that Debby completed ET before rapidly crossing the North Atlantic. However, near the UK ex-Debby started to lose its cold core and asymmetric structure typical to an extratropical cyclone. Ex-Debby phased back to warm cored while crossing Sweden, and at the same time it was rapidly deepening up to 27 hPa in 24 hours defining the storm as a meteorological bomb. Ex-Debby developed a frontal structure along a pre-existing cold front before hitting Lapland. It merged with the pre-existing low pressure center from the Norwegian Sea and proceeded right ahead of an upper trough, a region for cyclogenesis. These made the storm, now named Mauri, more intense as it crossed Lapland, and led to 30 m/s winds based on Finnish Meteorological Institute. Meanwhile, an occluded bent-back front approached Mauri, wrapped around the storm trapping the warmer air inside it and formed a warm seclusion. Due to that, Mauri regained the symmetric structure before reaching the Barents Sea.

Examining the climatic aspect, positive surface pressure and temperature anomalies over central Europe caused the jet stream to shift northward. Also, positive NAO and AO phases changed the storm track in general to higher latitudes. Hence, climatic conditions favoured the storm track to move more north.

The results of this thesis suggested that Mauri was the remnant of a hurricane Debby. It was shown that ERA-Interim was successful in locating the evolution of a cyclone and analysing its structure whereas it underestimated the surface pressure and wind speed values. Future work is still needed, for instance comparing these results to different reanalyses and collecting a statistic examination of hurricane originated storms in Europe, in order to adapt these methods and climatic indicators to future cases and storm predictions.

Avainsanat – Nyckelord – Keywords

Extratropical transition, hurricane Debby, storm Mauri, ERA-Interim, reanalysis

Säilytyspaikka – Förvaringställe – Where deposited

Kumpula campus library

Muita tietoja – Övriga uppgifter – Additional information

HELSINGIN YLIOPISTO
HELSINGFORS UNIVERSITET
UNIVERSITY OF HELSINKI

Tiedekunta/Osasto Fakultet/Sektion – Faculty		Laitos/Institution– Department
Matemaattis-luonnontieteellinen tiedekunta		Fysiikan laitos
Tekijä/Författare – Author		
Terhi Laurila		
Työn nimi/Arbetets titel – Title		
Syyskuun 1982 Mauri-myrskyn hurrikaaniperäisyys ja sen meteorologiset piirteet		
Oppiaine /Läroämne – Subject		
Meteorologia		
Työn laji/Arbetets art – Level	Aika/Datum – Month and year	Sivumäärä/ Sidoantal – Number of pages
Pro gradu	4/2016	51

Tiivistelmä/Referat – Abstract

Raju Mauri-myrsky iski Lappiin 22.9.1982 aiheuttaen 3 Mm^3 metsävauriot ja kaksi kuolonuhria. Maurin ajateltiin olevan peräisin 4-luokan Debby-hurrikaanista, mutta Debbyn ja Maurin välistä linkkiä sekä yhteyksiä ilmastollisiin olosuhteisiin ei ole tutkittu aiemmin.

Tässä työssä verrattiin syyskuun 1982 ilmastollisia oloja vuosien 1981-2010 syyskuihin. Laskelmat perustuvat Euroopan keskipitkien sääennusteiden keskuksen tuottamaan ERA-Interim-uusanalyysiin. ERA-Interimin myrskyrata on tehty Debbyn esiintymisestä Maurin Suomen ylitykseen saakka. Vertailun vuoksi Debbyn reitti on esitetty myös Yhdysvaltain liittovaltion sää- ja valtamerentutkimus-organisaation myrskyradan avulla. Työssä tarkasteltiin hurrikaani-Debbyn muuntumista keskileveys-asteiden matalapaineeksi sekä Mauri-myrskyn synoptista kehittymistä. Muuntuminen määriteltiin alkamaan myrskyn menettäessä hurrikaanin silmän symmetrisyyden muodostaessa rintamarakenteen, ja muuntuminen päättyy myrskyn ytimen muuttuessa lämpimästä kylmäksi. Mauria verrattiin myös kahteen muuhun voimakkaaseen, Euroopassa vaikuttaneeseen myrskyyn.

Työssä selvitettiin, että Debby muuntui keskileveysasteiden matalapaineeksi ennen kuin se ylitti nopeasti Pohjois-Atlantin. Lähellä Englantia ex-Debby alkoi kuitenkin menettää keskileveysasteiden myrskyille tyypillistä kylmän ytimen ja epäsymmetrisyyden rakennetta. Ex-Debby muuntui takaisin lämminytimiseksi ylittäessään Ruotsia samalla nopeasti syventyen jopa 27hPa/vrk määrittäen myrskyn meteorologiseksi pommiksi. Ex-Debby muodosti rintamarakenteen jo olemassa olevaan kylmään rintamaan ennen iskemistään Lappiin. Se yhdistyi Norjanmerellä olevan toisen matalapaineen keskuksen kanssa ja eteni yläsolan edelle, joka syventää pintamatalapainetta. Nämä voimistivat myrskyä entisestään, kun se kulki Lapin yli ja nimettiin Mauriksi, ja johtivat Ilmatieteen laitoksen havaintojen mukaan 30 m/s tuulen nopeuksiin. Tällöin taaksetaipunut okluusiorintama lähestyi Mauria, kiertyi sen ympärille vangiten lämpimämmän ilman myskyn keskuksen sisään ja muodosti lämpimän sekluusion. Tämän johdosta Mauri sai takaisin symmetrisen rakenteen ennen ajautumistaan Barentsinmerelle.

Ilmastollista näkökulmaa tutkiessa saatiin selville, että positiiviset pintapaine- ja lämpötila-anomaliat keski-Euroopan yllä aiheuttivat suihkuvirtauksen siirtymisen pohjoisemmaksi. Myös positiiviset NAO- ja AO-vaiheet muuttivat myrskyrataa yleisesti korkeammille leveys-asteille. Näin ollen ilmastolliset olosuhteet suosivat myrskyradan siirtymistä pohjoisemmaksi.

Työn tulokset viittavat siihen, että Mauri oli Debby-hurrikaanin jäänne. ERA-Interim onnistui matapaineen paikantamisessa, sen kehityskulun seuraamisessa ja myrskyn rakenteen tarkastelussa, kun se taas aliarvioi myrskyn pintapaineen ja –tuulen arvot. Tulevaisuudessa tämän työn tuloksia voisi verrata eri uusanalyyseihin, ja Euroopan hurrikaaniperäisistä myrskyistä olisi hyvä kerätä tilastollinen tarkastelu, jotta tämän työn menetelmiä ja ilmastollisia mittareita voisi soveltaa tulevaisuuden myrskytapauksiin ja sääennusteisiin.

Avainsanat – Nyckelord – Keywords
Myrskyn muuntuminen, Debby-hurrikaani, Mauri-myrsky, ERA-Interim, uusanalyysi
Säilytyspaikka – Förvaringställe – Where deposited
Kumpulan tiedekirjasto
Muita tietoja – Övriga uppgifter – Additional information

TABLE OF CONTENTS

1. INTRODUCTION 1
2. BACKGROUND 2
2.1. Development of tropical cyclones 3
2.2. Development of extratropical cyclones 3
2.2.1 Meteorological bomb 6
2.3. Differences between Tropical and Extratropical Cyclones 6
2.4. Extratropical transition 7
2.5. Meteorological measures and climate indices 9
2.5.1 Vorticity 9
2.5.2 Vorticity advection in the jet stream 10
2.5.3 El Niño – Southern Oscillation 13
2.5.4 North Atlantic Oscillation 13
2.5.5 Arctic Oscillation 14
3. DATA AND METHODS 14
3.1. ERA-Interim reanalysis data 14
3.2. Method for cyclone tracking 15
3.3. Methods for analysing extratropical transition 15
3.4. Hurricane track by NOAA 17
3.5. Reports and archives about Mauri 17
3.6. Climate indices data 18
4. RESULTS 19
4.1. Climatic conditions 19
4.2. Development of hurricane Debby 23
4.3. Storm track based on ERA-Interim and NOAA 24
4.4. Extratropical transition 27
4.4.1 Extratropical transition onset 27
4.4.2 Extratropical transition completion 28
4.4.3 Phase diagram 30
4.5. Vertical PV distribution 31
4.6. Development of storm Mauri 33
4.7. Comparison to other storms 38
5. DISCUSSION 40
6. CONCLUSIONS 44
ACKNOWLEDGEMENTS 46
REFERENCES 46

1. INTRODUCTION

On the 22nd of September 1982 an intense storm named Mauri travelled over Finland. The impacts were catastrophic toppling 3 million cubic meters of forest in Lapland, Northern Finland and causing two fatalities. At that time, the weather alerting system was insufficient, and there was no clear warning for the public about the upcoming intense storm. The case of Mauri was widely covered in the media but no peer-reviewed scientific articles have been published about it. There were thoughts whether Mauri was actually a remnant of hurricane Debby and had tropical characteristics that differ from typical extratropical cyclones but those were never investigated. Thus, these are the main research questions that will be determined in this thesis. The origin and evolution of storm Mauri will be examined as well as the factors that affected the development of the storm.

Intense storms like Mauri are rare in Finland. Research on these phenomena is challenging as knowledge about both the storm and its origin are needed. In addition to that, in order to improve weather and climate models, the capability of the models to detect and predict these storms have to be known. This case study of storm Mauri will try to find some possible mechanisms and climatological indicators for further investigation in future research.

In this thesis, *section 2* presents background for development of tropical and extratropical cyclones as well as the stages for a tropical cyclone to transform into an extratropical one. Also, meteorological measures and climate indices ENSO, NAO and AO, which are used to investigate the climatological aspect, are described. In addition, climate change effect on tropical and extratropical cyclones is shortly introduced. In *section 3*, ERA-Interim data, methods and other material are provided. In *section 4*, the results concerning propagation of hurricane Debby, its extratropical transition into storm Mauri and prevailing climatological conditions are presented. Debby and Mauri case is also compared to two other intense storms that have affected Europe. In *sections 5* and *6* discussion and conclusions of this thesis are provided.

2. BACKGROUND

The tropics (30°S – 30°N) obtain much more incoming solar energy than higher latitudes, and it causes meridional temperature differences (Holton & Hakim, 2013). Balancing that difference, warmer air from the tropics is transferred towards the polar regions and the large-scale movement of air, referred to as the atmospheric circulation, occurs. The annual-mean pole-to-equator temperature difference over the troposphere is typically 40 °C (Marshall & Plumb, 2007). The atmosphere in the tropics is generally barotropic, meaning that the density depends only on the pressure (Holton & Hakim, 2013).

The extratropics (30°S – 90°S and 30°N – 90°N) have regions where the temperature at a certain pressure level can change rapidly over short distance (Holton & Hakim, 2013). These regions, where density depends on both the temperature and the pressure, are called baroclinic. Baroclinic regions form in zones between two air masses where the temperature gradients are strong. The horizontal temperature gradient causes tilting of the pressure surfaces and therefore leads to the vertical shear of geostrophic wind, i.e the thermal wind. Baroclinic instability is the main mechanisms for extratropical cyclones to occur (Lin, 2007).

Tropical cyclones can travel to the extratropics, generally to the mid-latitudes (30°S – 60°S and 30°N – 60°N), and a tropical cyclone can undergo extratropical transition during which it obtains extratropical characteristics and turns into an extratropical cyclone (Hart & Evans, 2001). The great temperature difference between tropical and polar air masses causes pressure differences and it is balanced by jet streams which are the strongest at the meeting zone of different air masses (Holton & Hakim, 2013). Available potential energy in a baroclinic atmosphere is stored in the mean flow (Lin, 2007). Baroclinic instability releases available potential energy and converts it into perturbation kinetic energy which can cause the growth of small disturbances. These disturbances can further develop to become extratropical cyclones. Extratropical cyclones are responsible for most of the meridional transport of energy in the mid-latitudes (Holton & Hakim, 2013).

The key components that need to be explored, when investigating extratropical transition, are described in more detail. In order to examine the climatological conditions in September 1982, some climate indices are presented as well.

2.1. Development of tropical cyclones

Tropical cyclones are intense rotating storms that originate over tropical oceans (Holton & Hakim, 2013). Depending on the location, storms are referred to hurricanes (the North Atlantic Ocean and the eastern North Pacific Ocean), typhoons (the western North Pacific Ocean) or tropical cyclones (the western South Pacific Ocean and the Indian Ocean). The main energy source of a tropical cyclone is the latent heat release of condensation which is mostly needed to maintain convection (Miller, 1985). For the tropical cyclone to have enough energy for development the ocean temperatures must be at least about 26-27 °C (Palmén, 1948). Also, the vertical wind shear has to be low so that the heating can be vertically aligned causing the air to rise high (Holton & Hakim, 2013). The Saffir-Simpson hurricane wind scale (*Table 1*) rates hurricanes to categories from 1 to 5 based on 1-minute sustained wind speed. The scale is a good tool for alerting people and provides estimations of damage (Schott, et al., 2012).

Table 1. *The Saffir-Simpson Hurricane Wind Scale.*

Category	1-min Winds (m/s)	Estimated Damage
1	33-42	Some damage
2	42-49	Extensive damage
3	49-58	Devastating damage
4	58-69	Catastrophic damage
5	> 69	Catastrophic damage

2.2. Development of extratropical cyclones

The development of extratropical cyclones is usually referred to as cyclogenesis (Holton & Hakim, 2013). There are two typical models that describe cyclogenesis: The

Norwegian cyclone model and The Shapiro-Keyser model (Schultz, et al., 1998). The Norwegian cyclone model, also known as the polar front theory of cyclogenesis, was developed by Bjerknes (1919) and Bjerknes and Solberg (1922), and presents the structure and evolution of extratropical cyclones. It was based on observed fronts in North-West Europe. In the Norwegian model, the development of a cyclone begins with a disturbance in a region of a strong temperature gradient (*Figure 1a, stage I*) i.e. in the baroclinic zone along the polar front (Bjerknes & Solberg, 1922). The cyclonic circulation of the disturbance forms a narrow, lengthy cold front, a broad, short warm front, a low pressure center, and a warm sector between the fronts (*Figure 1a, stage II*). The low strengthens, colder air starts to slide underneath warmer air at the fronts and rising air forms clouds and precipitation (*Figure 1a, stage III*). The cold front rotates faster than the warm front and therefore it reaches the warm front and they merge to form an occluded front (*Figure 1a, stage IV*). The jet stream flows above the occlusion point. The forming occluded front suppresses the supply of warm air from the low pressure center causing the cyclone to dissipate.

The Shapiro-Keyser model was proposed later by Shapiro and Keyser (1990), and it is based on observations of fronts in the North-East USA. In this model a cyclone begins to develop like in the Norwegian model, as a disturbance on a baroclinic zone (*Figure 1b, stage I*) (Schultz, et al., 1998). However, instead of the cold front overtaking the warm front, in the Shapiro-Keyser model the cold front moves almost perpendicular to the warm front (*Figure 1b, stage II).* That structure is called the frontal T-bone. A fracture occurs in the magnitude of the horizontal temperature gradient along the cold front near the low center (*Figure 1b, stage III*). A bent-back front, an occluded front that reverses its direction of motion, develops as the poleward portion of the cold front weakens. Eventually, the low center gets wrapped around by the bent-back front closing warmer air inside and forming a warm seclusion (*Figure 1b, stage IV*). It is known (Browning, 2004) that if the central pressure of a cyclone deepens during the warm seclusion phase, it produces severe surface winds.

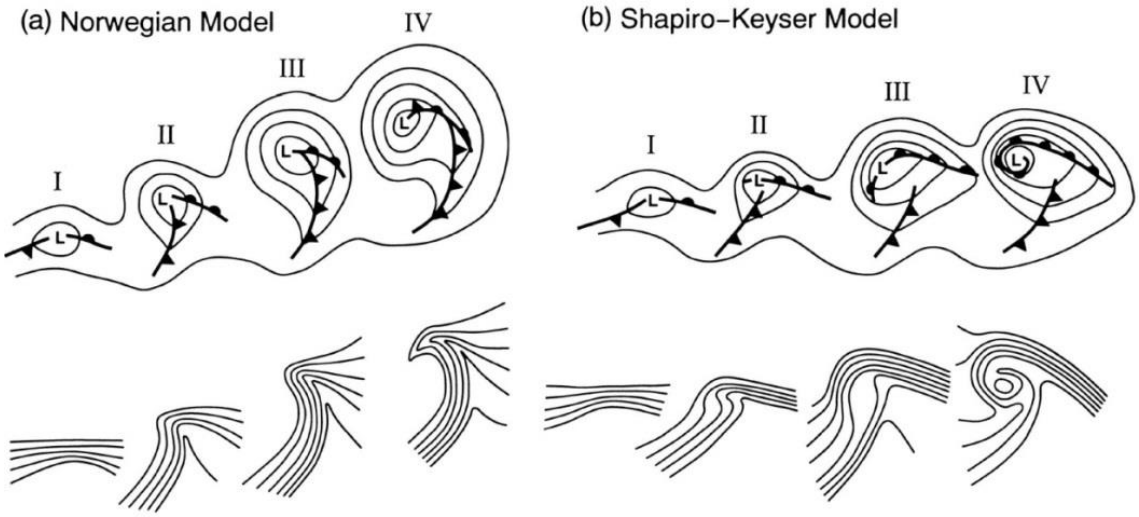

Figure 1. *Conceptual models of cyclone evolution showing low-level geopotential height and fronts (top), and low-level potential temperature (bottom).* (Schultz, et al., 1998)
(a) *Norwegian cyclone model: (I) incipient frontal cyclone, (II) and (III) narrowing warm sector, (IV) occlusion;*
(b) *Shapiro-Keyser cyclone model: (I) incipient frontal cyclone, (II) frontal fracture, (III) frontal T-bone and bent-back front, (IV) frontal T-bone and warm seclusion. (b) is adapted from Shapiro and Keyser (1990), their FIG. 10.27, to enhance the zonal elongation of the cyclone and fronts and to reflect the continued existence of the frontal T-bone in stage IV.*
The stages in the respective cyclone evolutions are separated by approximately 6-24 h and the frontal symbols are conventional. The characteristic scale of the cyclones based on the distance from the geopotential height minimum, denoted by L, to the outermost geopotential height contour in stage IV is 1 000 km.

The Norwegian cyclone model applies typically to cyclones embedded in diffluent, high-amplitude background flow, and the Shapiro-Keyser model is more applicable in confluent, low-amplitude zonal flow (Schultz, et al., 1998). The Norwegian cyclone tends to have a strong cold front and weak warm front when the Shapiro-Keyser cyclone has weak cold front and strong bent-back warm front. The Norwegian model applies best for extratropical cyclones over continental landmasses, especially for the low pressure systems near the eastern parts of the North Atlantic, whereas the Shapiro-Keyser model applies best for oceanic extratropical cyclones.

2.2.1 Meteorological bomb

An extratropical cyclone is defined as a meteorological bomb if its central pressure deepens rapidly (Sanders & Gyakum, 1980). The phenomenon is also referred to explosive development, explosive cyclogenesis or bombogenesis. Sanders and Gyakum (1980) took the effect of latitude into account, and defined a meteorological bomb by a fall of more than

$$1 \frac{hPa}{hour} * \frac{\sin \varphi}{\sin 60°}, \quad (1)$$

where φ is latitude, of a cyclone's minimum sea level pressure over a period of at least 24 hours. The bomb is characterized with a major head cloud mass that appears in satellite imagery in the early stage of deepening (Böttger, et al., 1975). Explosive development is usually located downstream of an upper level trough, within or poleward of the maximum westerlies and within or ahead of the planetary-scale troughs (Sanders & Gyakum, 1980). As the central pressure of a meteorological bomb is extremely low, hence, the horizontal gradient in sea level pressure is also greatly large. That leads to damaging surface winds.

2.3. Differences between Tropical and Extratropical Cyclones

A tropical cyclone is defined as a non-frontal (*Figure 2a*), warm core (*Figure 2b*) cyclone that originates in the tropics (Elsberry, 1995). It has symmetrical structure, an eye and an eye wall (Jones, et al., 2003). Precipitation is convective and it forms spiral bands. Diabatic PV has its maximum anomalies in the lower troposphere. Sea surface temperature (SST) has a significant role in tropical cyclone development since the energy for the tropical cyclone comes from latent heat release (Miller, 1985). Maximum wind speeds occur just outside the eye near the surface and occur to the right of the cyclone track in the Northern Hemisphere (Powell, 1982).

An extratropical cyclone has asymmetrical structure with fronts (*Figure 2c*) and a cold core (*Figure 2d*) (Klein, et al., 2000). Geopotential surfaces are tilted rearwards with height. Extratropical cyclones develop in the mid-latitudes where horizontal

temperature gradients are large. Precipitation is mostly aligned along the fronts, and PV anomalies are strongest at upper levels. Maximum wind speeds occur usually at upper levels away from the cyclone center.

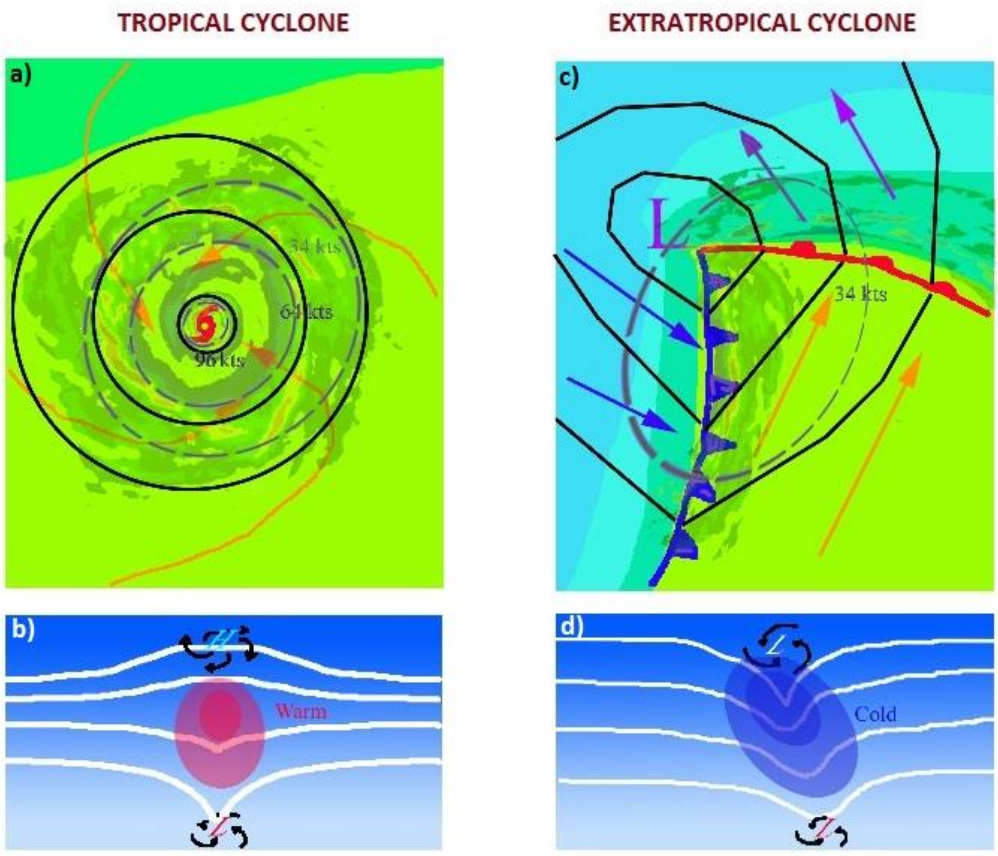

Figure 2. *Top panel: Maps of temperature (shaded), wind field (dashed lines) and geopotential (contoured) associated with* ***(a)*** *a tropical cyclone and* ***(c)*** *an extratropical cyclone. Colors indicate temperature (blue=15°C, blue green=20°C, green=25°C).*
Bottom panel: Maps of the vertical structure for ***(b)*** *a tropical cyclone and* ***(d)*** *an extratropical cyclone. The contours are geopotential surfaces and temperature is shaded with schematic of the circulation overlaid. Figure modified based on* Merril *(*1993*).*

2.4. Extratropical transition

On average, 46 % of Atlantic tropical cyclones (Hart & Evans, 2001) and 27 % of western North Pacific tropical cyclones (Klein, et al., 2000) complete extratropical transition (ET). Coastal Western Europe is likely to be impacted by transitioning tropical

cyclones once every one to two years (Hart & Evans, 2001). The North Atlantic hurricane season is officially from the 1st of June to the 30th of November, and ET is most likely late in the season due to more equatorward positioned jet stream, with October having the highest probability of transition (50 %). The highest occurrence for Atlantic ET is at lower latitudes (30°N - 35°N) early and late in the hurricane season and at high latitudes (40°N - 50°N) during the peak of the season (Hart & Evans, 2001).

ET does not have one accepted definition (Malmquist, 1999). Evans and Hart (2003) define that the ET onset occurs when the storm becomes consistently asymmetric. The storm symmetry is measured by the storm-relative right minus left asymmetry in the thickness field,

$$B = h\left[\left(\overline{Z_{600} - Z_{900}}\right)_{right} - \left(\overline{Z_{600} - Z_{900}}\right)_{left}\right], \quad (2)$$

where B is defined as a natural indicator of storm symmetry, h denotes the hemisphere (1 = Northern Hemisphere, -1 = Southern Hemisphere), Z refers to geopotential height, and the overbar indicates the areal mean over the semicircle with respect to the storm motion. The 900-600 hPa layer represents the lower troposphere. The suitable area for B should include the convergent circulation of a tropical cyclone but not extend into other systems not affecting the cyclone (Evans & Hart, 2003). An average radius of a moat, a region between an eye wall and an outer rain band, is 4°-6° (Frank, 1977). Therefore a radius of 500 km, which is about 5° in the east coast of the USA, has been chosen. Also Hart (2003) has confirmed the 500 km radius to be an appropriate horizontal region for describing the storm evolution by investigating a dataset of 61 storms and dozens of mid-latitude systems.

The completion of ET is defined when the storm has become cold cored (Evans & Hart, 2003). It is defined by the thermal wind field,

$$\frac{\partial(Z_{\mathrm{MAX}} - Z_{\mathrm{MIN}})}{\partial \ln p}\Bigg|_{900\ \mathrm{hPa}}^{600\ \mathrm{hPa}} = -V_T^L, \quad (3)$$

where Z_{MAX} and Z_{MIN} are the maximum and minimum geopotential heights within 500 km of the cyclone and V_T^L is the thermal wind in the lower troposphere. In a cold core

cyclone the geostrophic wind speed increases with height, and hence ET is completed when V_T^L first becomes negative.

When a tropical cyclone moves to higher latitudes it is influenced by the mid-latitude environment: baroclinicity and vertical shear increases, meridional humidity gradients form, SST decreases, SST gradients strengthen and the Coriolis parameter becomes larger (Klein, et al., 2000). All the environment changes lead to asymmetric appearance and gradually loss of the warm core. Cut-off from the warm SSTs causes a decrease in tropical cyclone intensity; however, during ET the cyclone starts to accelerate under the increasing influence of the mid-latitude westerly jet stream. A tropical cyclone might decay in the tropics and not complete the transformation. For a tropical cyclone to re-intensify as an extratropical cyclone, it must interact with an upper level trough and positive PV anomaly; otherwise there is no forcing for ascent. If the interaction occurs, the cyclone develops extratropical characteristics such as fronts and vertical tilt. It can then either re-intensify as an extratropical cyclone or decay depending on the mid-latitude environment.

2.5. Meteorological measures and climate indices

2.5.1 Vorticity

Vorticity is a measure of local rotation in a fluid (Holton & Hakim, 2013). Cyclonic (anticyclonic) rotation is defined as positive (negative) vorticity in Northern Hemisphere. Potential vorticity (PV) takes into account thermodynamic limitations on the motion and therefore it's useful for interpreting atmospheric dynamics. The potential vorticity unit (PVU) is defined as

$$1\ PVU = 10^{-6}\mathrm{K\,kg^{-1}m^2s^{-1}}. \quad (4)$$

PV has higher values in the stratosphere and polar regions and lower values in the troposphere due to the change of the static stability. Typically the 2 PVU surface is considered to be the dynamic tropopause.

PV represents the potential to change vorticity by changing either the latitude or the static stability,

$$PV = -g(\zeta + f)\frac{\partial \theta}{\partial p} \ , \tag{5}$$

where g is gravitational acceleration, ζ is relative vorticity, f is the Coriolis parameter, θ is potential temperature and p is pressure. The sum of relative vorticity and Coriolis parameter is defined as absolute vorticity ($\eta = \zeta + f$) and $\partial\theta/\partial p$ describes the static stability. Relative vorticity refers to the circulation of weather systems and it consists of curved flow and wind shear (Holton & Hakim, 2013). Absolute vorticity is the sum of Earth vorticity represented by Coriolis parameter and relative vorticity.

PV is conserved following adiabatic, frictionless flow (Holton & Hakim, 2013). For example, if stability $\partial\theta/\partial p$ decreases, absolute vorticity $\eta = \zeta + f$ must increase to conserve PV. However, when a process is diabatic or frictional, PV is not conserved. Above the diabatic heating, static stability decreases, divergence leads to a decrease in vorticity, and hence PV decreases. In contrast, below the heating maximum, PV increases. Typically diabatic heating is the greatest in the mid-troposphere. Therefore, in an area of diabatic heating, positive PV anomaly occurs in the lower troposphere and negative PV anomaly in the upper troposphere. Cyclonic (anticyclonic) PV anomaly induces a cyclonic (anticyclonic) circulation (Hoskins, et al., 1985).

2.5.2 Vorticity advection in the jet stream

If horizontal advection of air masses is not spatially uniform then regions of convergence and divergence will occur. To satisfy the continuity equation, vertical motion of air must exist. When there is convergence at the surface, ascent occurs, and divergence at the surface leads to decent (*Figure 3*). Rising air combined with moisture is associated with clouds and precipitation and sinking air leads usually to clear conditions. When winds at the surface are cyclonic, convergence occurs and low pressure develops. A region of strong divergence at the upper levels enhances a cyclone to intensify.

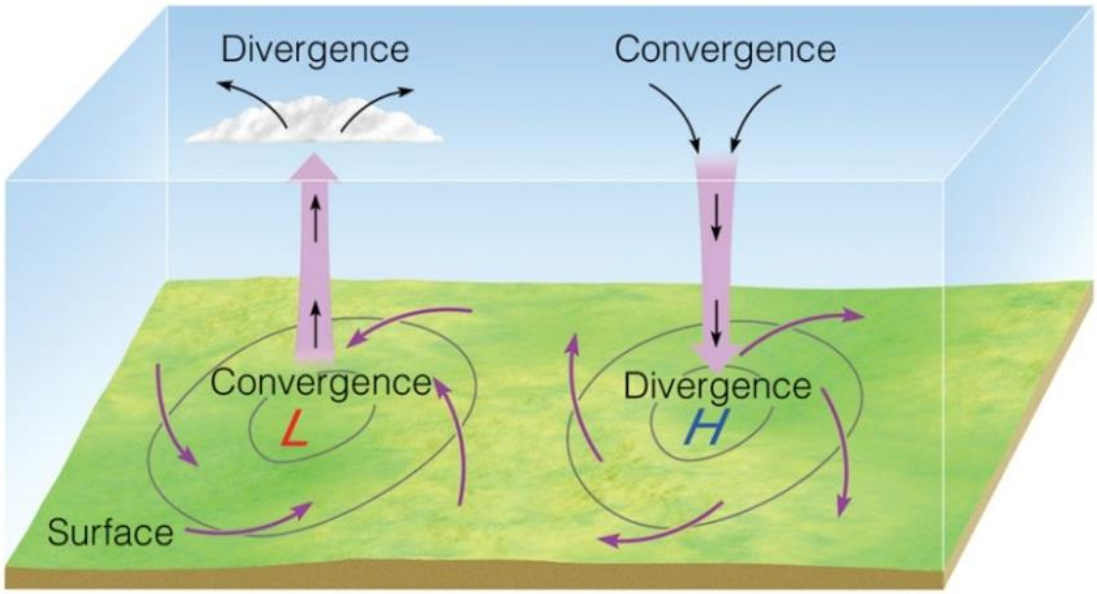

Figure 3. *Horizontal divergence and convergence, and vertical motion of air. Figure from* (Ahrens, 2012).

In the entrance region of a jet stream the wind accelerates and ageostrophic wind causes upper level divergence on the right side of jet entrance (Uccellini, 1990). In the exit region, the wind decelerates and the resulting ageostrophic wind results in divergence on the left side of jet exit. If there is divergence at upper levels there must be convergence at the surface, and hence ascent results. *Figure 4* shows how these regions and vorticity maximum and minimum are located in the jet stream.

Wavelike jet streams form upper level ridges and troughs. As the jet stream is moving, it causes relative vorticity anomalies. Positive vorticity advection (PVA) results when air from a region of positive vorticity advects to a region of negative vorticity. In the jet stream, PVA occurs upstream of a ridge axis and downstream of a trough axis (*Figure 5*). In the area of PVA its most intense values are located right ahead of the trough. Negative vorticity advection (NVA) appears when air is moving from a region of negative vorticity to a region of positive vorticity. NVA occurs upstream of a trough axis and downstream of a ridge axis.

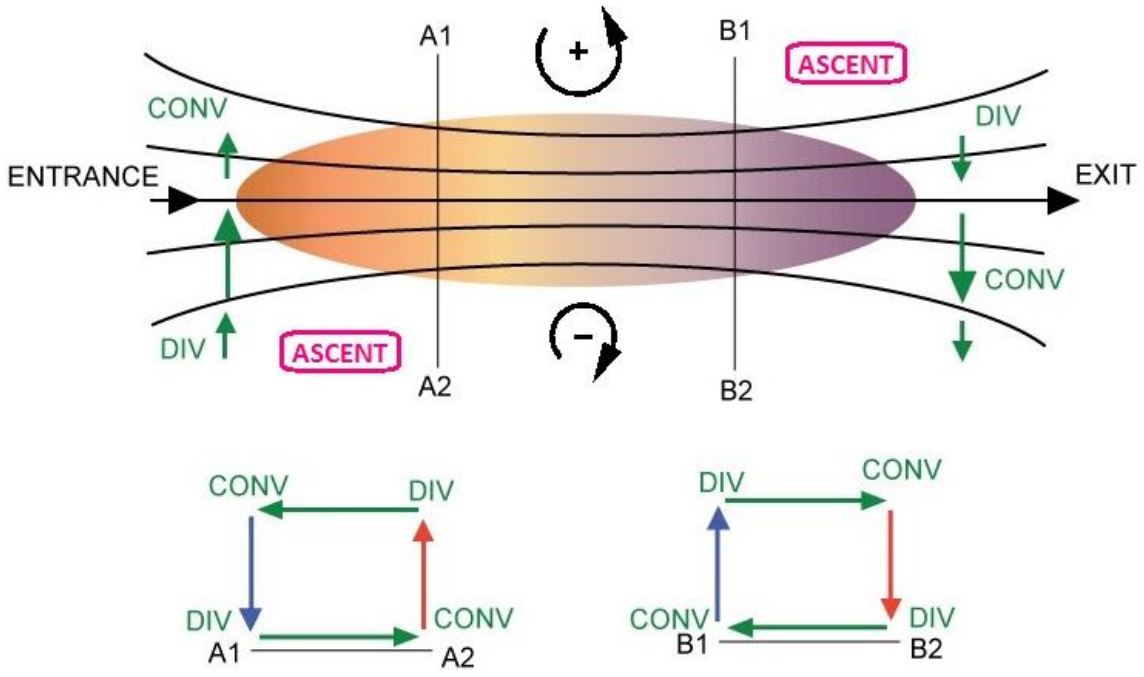

Figure 4. *Jet entrance and exit regions associated with convergence and divergence, regions of ascent, and vorticity maximum (+) and minimum (-). Figure modified based on* (Kocin & Uccellini, 1987).

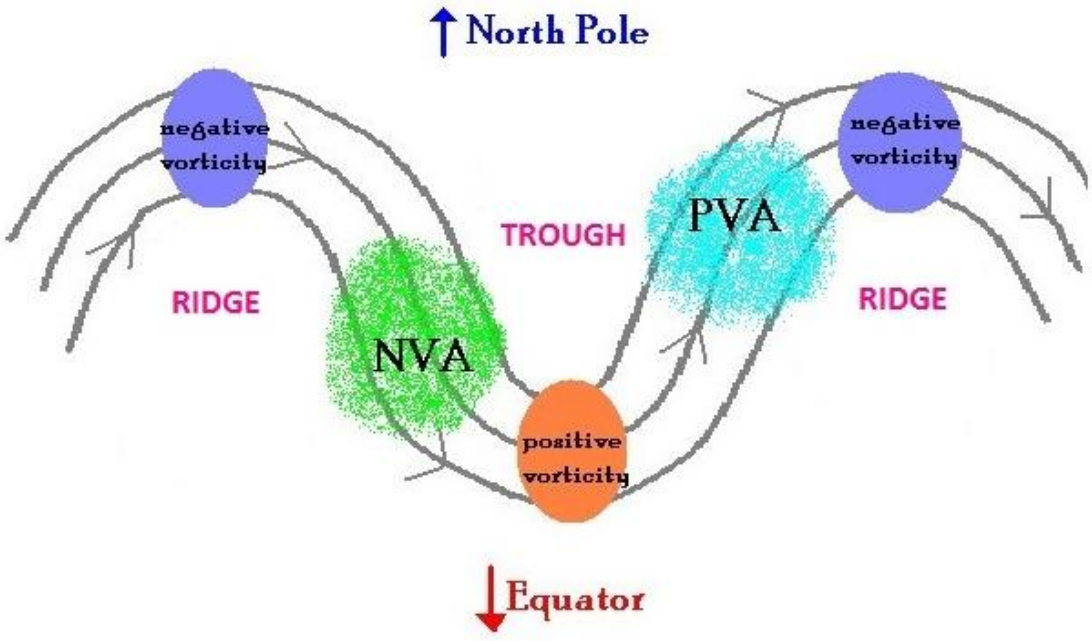

Figure 5. *A jet stream with streamlines (grey lines), negative vorticity (purple) and positive vorticity (orange), regions of positive vorticity advection (PVA, turquoise) and negative vorticity advection (NVA, green), and trough and ridges (pink writing). Figure modified based on University of Wisconsin-Madison, AOS 101 Weather and Climate, lecture note.*

2.5.3 El Niño – Southern Oscillation

The zonal pressure gradient in the tropics has an irregular inter-annual variation (Holton & Hakim, 2013). This so called Southern Oscillation causes changes in patterns of wind, temperature and precipitation. When the pressure difference between Darwin and Tahiti is small, the weakening of trade winds reduces oceanic upwelling and deepens the thermocline in the eastern Pacific. This leads to an increase in SSTs and is called El Niño. The opposite phase, where strong pressure difference leads to decrease in SST, is referred to as La Niña. The entire phenomenon is named El Niño – Southern Oscillation (ENSO). El Niño appears every two to seven years (NOAA Warm Episodes, 2012).

During El Niño (positive ENSO phase) there is an anomalous increase in upper tropospheric westerly winds over the equatorial Atlantic and the Caribbean basin (Gray, 1984). These strong winds increase tropospheric vertical wind shear and inhibit tropical cyclone activity. In general, reduced tropospheric vertical wind shear is associated with increased cyclone activity and stronger shear with decreased activity. (Goldenberg & Shapiro, 1996). Hence, there is a significant correlation between warm (cold) ENSO phase and the decrease (increase) in Atlantic tropical cyclone frequency (Gray, 1984). During El Niño also the storm tracks in mid-latitudes differ significantly from the normal paths causing temperature and precipitation anomalies in many regions (NOAA Warm Episodes, 2012).

2.5.4 North Atlantic Oscillation

The North Atlantic Oscillation (NAO) refers to the variation of pressure anomalies between the Azores and Iceland (Walker, 1924). In the positive NAO phase, the subtropical Azores high pressure center is abnormally stronger and the subpolar Icelandic low pressure center is deeper. This increased pressure gradient causes strong westerly winds, and the North Atlantic jet stream shifts poleward (Vallis & Gerber, 2008) and its southwest-northeast tilt increases followed by the storm track of extratropical cyclones (Woollings, et al., 2010). During the negative NAO phase, high and low pressure centers are weak and extratropical cyclones are weaker than normal crossing on a more zonal pathway. NAO also affects extratropical transition; when the NAO index is positive,

the transition frequency is decreased (Hart & Evans, 2001). NAO exhibits inter-annual and inter-seasonal variability fluctuating from weeks to months and years to decades.

2.5.5 Arctic Oscillation

The pressure difference variability between the polar region and the northern mid-latitudes is referred to as Arctic Oscillation (AO) (Thompson & Wallace, 1998). When the atmospheric pressure is abnormally high in the Arctic, AO phase is positive. It leads to stronger North Atlantic westerly winds, and the storm track moves farther north. When the AO index is negative, the pressure gradient is small, and therefore westerly winds are weaker. Hence, extratropical cyclones develop on a more southern region. AO is closely related to NAO, and it varies with no particular periodicity.

3. DATA AND METHODS

3.1. ERA-Interim reanalysis data

The European Centre for Medium-Range Weather Forecasts (ECMWF) has produced a global atmospheric reanalysis called ERA-Interim (Dee, et al., 2011). It replaced ERA-40, the previous atmospheric reanalysis produced by ECMWF, and is continuously updated in real time. The spatial resolution of the ERA-Interim dataset is higher than in ERA-40, approximately 80 km horizontally. There are 60 vertical model levels and data can be interpolated from model levels to pressure levels. ERA-Interim covers the period from January 1979 onwards, and it uses a 4-dimensional variational data assimilation system (4D-Var). The reanalysis produces output in 6-hour intervals. It is shown (Hodges, et al., 2011) that extratropical cyclone characteristics are well matched between ERA-Interim and other new reanalyses, for example National Centers for Environmental Prediction – Climate Forecast System Reanalysis (NCEP-CFSR). The numbers and spatial distribution of extratropical cyclones correlate well between the reanalyses but the greatest differences occur in maximum intensities.

The dataset for this study is taken from the daily (every 6 hours) ERA-Interim fields in September 1982 as well as monthly means of daily means for the month of September. The latter are also collected from the year 1981 to 2010 in order to calculate the anomalies for 30 year period. The data includes mean sea level pressure, geopotential height, temperature, potential vorticity and zonal and meridional components of wind velocity. In this study the data is analysed on pressure levels which are available every 25 hPa from 1 000 hPa up to 750 hPa and 250 hPa up to 100 hPa, and every 50 hPa from 750 hPa up to 250 hPa.

3.2. Method for cyclone tracking

In this thesis, the cyclone tracking is based on locating the minimum value of sea level pressure and defining its coordinates to be the center of the cyclone. Since the location of hurricane Debby is already known quite accurately, the possible region to locate the cyclone is easier to limit. Therefore, the cyclone center is located by manually limiting the possible region near the known location, and a pre-existing, fully automatic cyclone tracking algorithm is not used. After finding the storm track of Debby, the cyclone is followed across the North Atlantic to Scandinavia in order to investigate the whole path and see the connection between hurricane Debby and storm Mauri.

3.3. Methods for analysing extratropical transition

The extratropical transition onset is calculated based on the B-index (see *equation 2, section 2.4*). B-index refers to the symmetry of the storm; when the value is less than 10, the cyclone is defined to be symmetric, on the contrary, values greater than 10 mean asymmetricity (Evans & Hart, 2003). The B-index is calculated from the thickness difference on the right and left side of the storm within 500 km radius. In this thesis, the geopotential heights at 600 hPa and 900 hPa are collected from the ERA-Interim reanalysis database, and the difference of the geopotential heights between the pressure levels is calculated at each time step (every 6 hours). After that, the 500 km radius is plotted centered on the low pressure center (*Figure 6a*). The line between the right and left side is drawn using the low pressure center locations at the time in question

and at the next time step. Then, the data points inside the 500 km radius are divided depending on the side of the line, and averages of the geopotential height differences on both the right and left areas are calculated. Lastly, the 600-900 hPa geopotential difference on the left side is subtracted from the right side, and the outcome is the B-index. The same process is repeated for each time step.

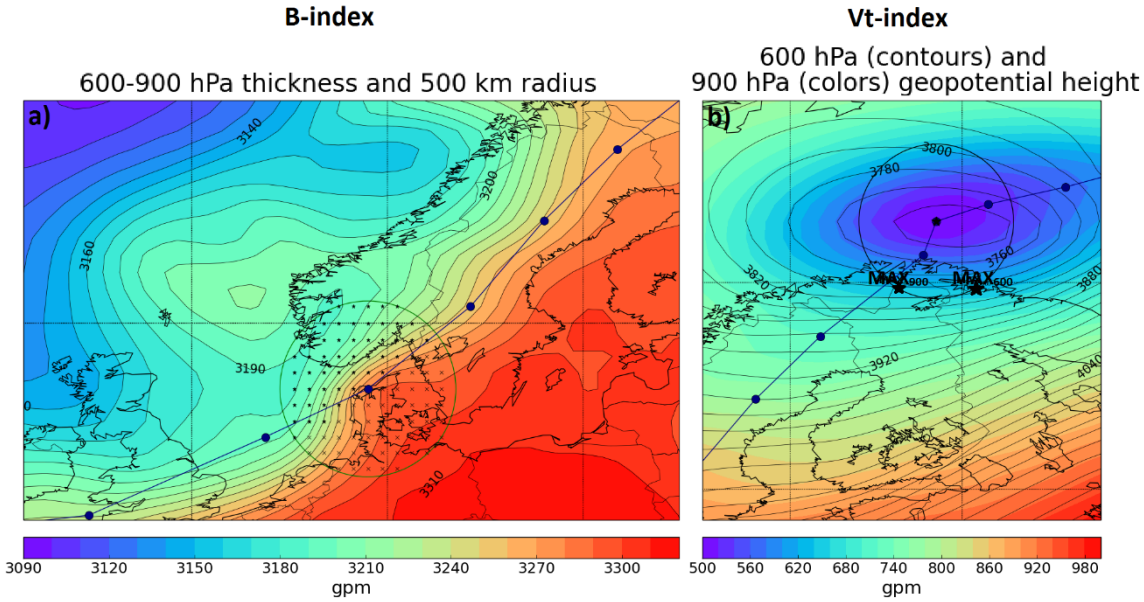

Figure 6. *Examples of calculated indices. The circle marks the 500 km radius from the low pressure center, and the dots along the line are the center of the cyclone every 6 hours.* ***a)*** *B-index on the 21st Sept 18Z. The crosses and stars inside the circle indicate whether the data point belongs to the right or left side of the line.* ***b)*** *Vt-index on the 23rd Sept 00Z. The stars with the label MAX indicate the locations of the maximum geopotential value at 900 hPa (left star) and 600 hPa (right star).*

The Vt-index indicates the time when the extratropical transition is completed by calculating the thermal wind in the vicinity of the low pressure center (see *equation 3, section 2.4*). The Vt-index refers to whether the cyclone is warm (positive values) or cold (negative values) cored (Evans & Hart, 2003). Geopotential heights at 600 hPa and 900 hPa are also used when calculating the Vt-index; at each time step from both pressure levels, the geopotential height value located at the center of the low pressure and the maximum geopotential height value within the 500 km radius from the center are

investigated (*Figure 6b*). Then, the geopotential height difference between the maximum and center values are calculated on both pressure levels separately, and the outcome at 900 hPa level is subtracted from the outcome at 600 hPa level. Lastly, the subtracted value is divided by the natural logarithm of the pressure difference between the levels. The result from this is the Vt-index which also refers to the thermal wind around the cyclone.

Phase diagrams are used for characterizing the phase and structure of cyclones (Hart, 2003). Based on a phase diagram the evolution and transition of a cyclone can be diagnosed. The parameters in a phase diagram describe the general structure of a cyclone; whether it has a warm core and vertically stacked nature of a tropical cyclone or a cold core and vertical tilt of an extratropical cyclone. These parameters are the lower-tropospheric thickness asymmetry (B–index) and the lower-tropospheric thermal wind (V_T–index). A phase diagram has the V_T–index on x-axis and the B–index on y-axis.

3.4. Hurricane track by NOAA

The National Oceanic and Atmospheric Administration (NOAA) produces track data of historical hurricane cases. The dataset is based on both AOML HURDAT2 reanalysis (Atlantic Oceanographic & Meteorological Laboratory Hurricane Data 2nd generation) and IBTrACS dataset (the International Best Track Archive for Climate Stewardship) (NOAA Data Registry, 2014). HURDAT2 reanalysis is an updated version of HURDAT reanalysis (Hurricane Database); a post-storm analysis of the intensity, central pressure, location and size of tropical and subtropical cyclones (Jarvinen, et al., 1984). IBTrACS is a collection of best track data and observations from different agencies and it provides global tropical cyclone data (Knapp, et al., 2010). IBTrACS includes best track data from 11 organizations. Hence, a hurricane track by NOAA is a combination of a reanalysis and many observations.

3.5. Reports and archives about Mauri

As storm Mauri occurred in 1982, there are limited measurements and data available. In addition, no peer-reviewed scientific articles have been published about this

storm. Therefore, some additional information was gathered from the reports and archives of Finnish Meteorological Institute (FMI). FMI has stored many newspapers with articles and footage of Mauri. They describe well the impact and magnitude of the storm. FMI has a press release from the 24th of September 1982 describing storm Mauri's weather conditions, predicted and measured wind speeds, reliability of the prediction and information about the weather alerting system of that time. There is also a description by a FMI meteorologist about weather conditions during Mauri dated on December 1982. In addition, there is a report from FMI to an ombudsman of the Finnish Parliament from the 3rd of December 1982 which includes extended information from the press release.

FMI has archived microfilms from the decades before computers were the main analyse tool. Microfilms include maps with synoptic observations and hand drawn isobars and fronts. These are available at levels 300 hPa, 500 hPa, 700 hPa, 850 hPa and at the surface every 6 hours. The maps cover the region over the North Atlantic and Europe. In this thesis microfilms are used only as a supportive and confirmative information source for other materials.

3.6. Climate indices data

All the climate indices for this study are collected from the Climate Prediction Center, NOAA. NOAA has calculated the ENSO index based on SST anomalies from the 3-month running average of ERSST.v4 dataset (Extended Reconstructed Sea Surface Temperature, version 4) in the Niño 3.4 region (5°N – 5°S, 170°W – 120°W) with the base period 1981–2010 (NOAA Monitoring & Data: Index Values, 2015).

The NAO index calculation is based on the Rotated Principal Component Analysis (RPCA) which is applied to monthly mean 500 hPa height standardized anomalies obtained from the Climate Data Assimilation System (CDAS) in the analysis region (20°N – 90°N, all longitudes) with the base period 1950–2000 (NOAA Teleconnection Index Calculations, 2015). The anomalies are standardized by the 1950-2000 period monthly means and standard deviations. The AO index is based on monthly mean 1000 hPa height standardized anomalies in the leading Empirical Orthogonal Function (EOF) mode in the

analysis region (20°N – 90°N, all longitudes) with the base period 1979–2000 (NOAA Teleconnection Pattern Calculation Procedures, 2015).

4. RESULTS

4.1. Climatic conditions

1982 was a year with an extremely low activity hurricane season; only two hurricanes occurred in the Atlantic Ocean (Clark, 1983). The last year before that with only two hurricanes was 1931 (Clark, 1983) and after 1982 there has been only one year, 2013, with just two hurricanes (NOAA News, 2014). The lack of hurricanes was partly attributed to the increase in upper level westerly winds and to the weakness of lower level easterly trade winds in the tropical North Atlantic. Furthermore, increased tropospheric vertical wind shear leads to decrease in tropical cyclone activity since the heating is not anymore vertically aligned causing convection to rise high. Increased vertical wind shear originates from a strongly positive El Niño phase (ENSO index +1.70 from September to November 1982) meaning weak pressure gradients between Darwin and Tahiti.

In September 1982, low mean sea level pressure (MSLP) values, down to 999 hPa, were located around Iceland and high values, up to 1024 hPa, over the central North Atlantic and central Europe (*Figure 7a*). This indicates a strongly positive NAO phase (NAO index +1.76 in September 1982) causing the storm track to shift poleward. A strong pressure gradient occurred along northern parts of the North Atlantic extending north-eastward to the UK and Scandinavia. Also, the AO phase was positive (AO index +0.558 in September 1982) meaning a stronger than normal pressure gradient between the polar regions and the mid-latitudes. As is the case for positive NAO phase, positive AO phase causes westerlies to increase due to the stronger pressure gradient and the storm track to move northward.

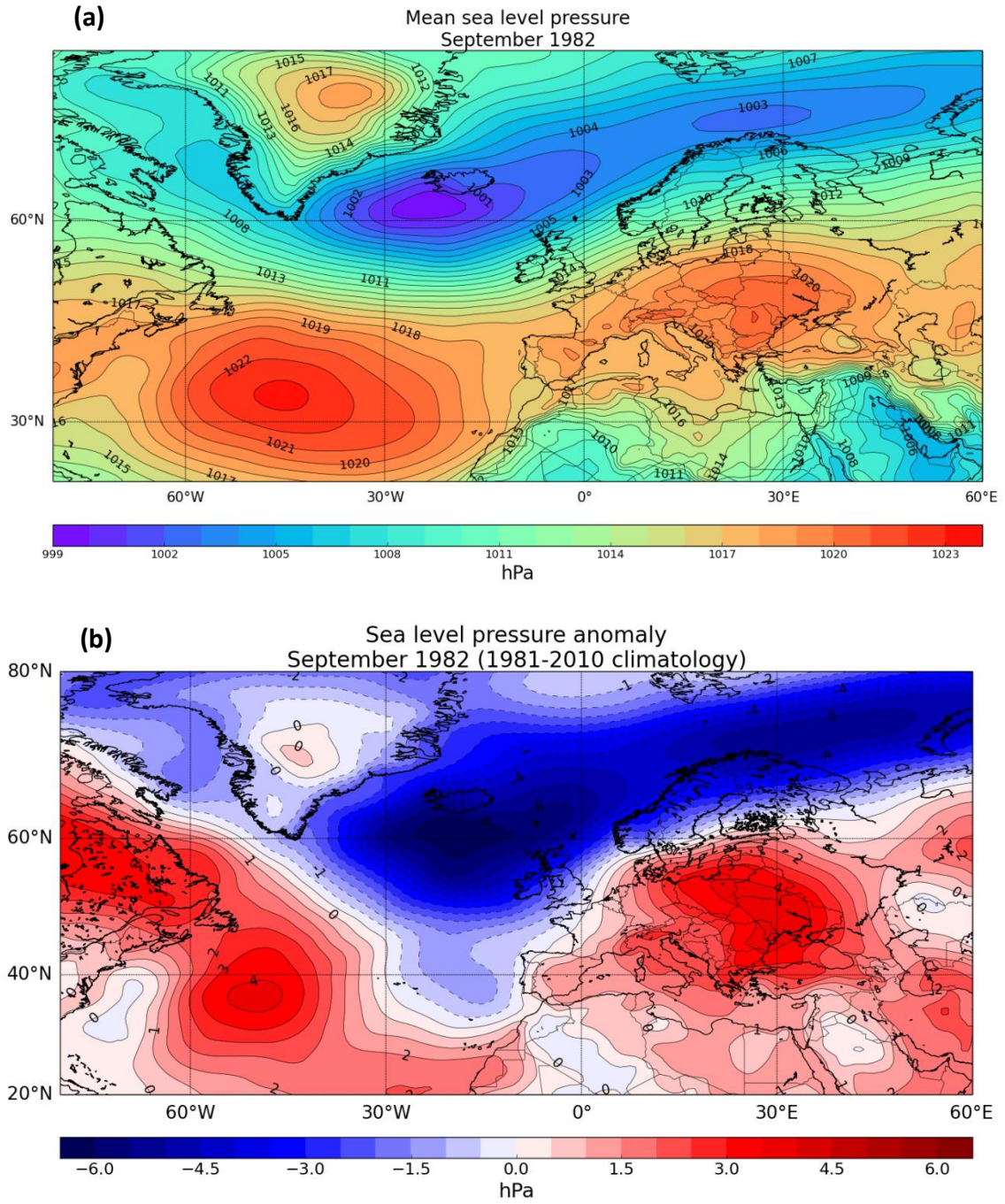

Figure 7. ***(a)*** *Mean sea level pressure (hPa) in September 1982, and* ***(b)*** *its anomaly (hPa, base period of September 1981-2010) based on ERA-Interim reanalysis.*

There was a strong high pressure area dominating over central Europe (*Figure 7a*), and it caused a positive MSLP anomaly with a magnitude of 3-5 hPa (*Figure 7b*). The high pressure created divergence at the surface, convergence at the upper levels and hence

the air was in sinking motion. That led to warm conditions over central Europe. Accordingly, temperatures were creating a strongly positive surface temperature anomaly with a magnitude of 4 degrees (*Figure 8*). The SST anomaly pattern was similar to the surface temperature (not shown). As the isobars were far apart, the mean surface winds were really weak (not shown) which indicated anomalous anticyclonic circulation in central Europe. All these features favoured the storm track to move more north.

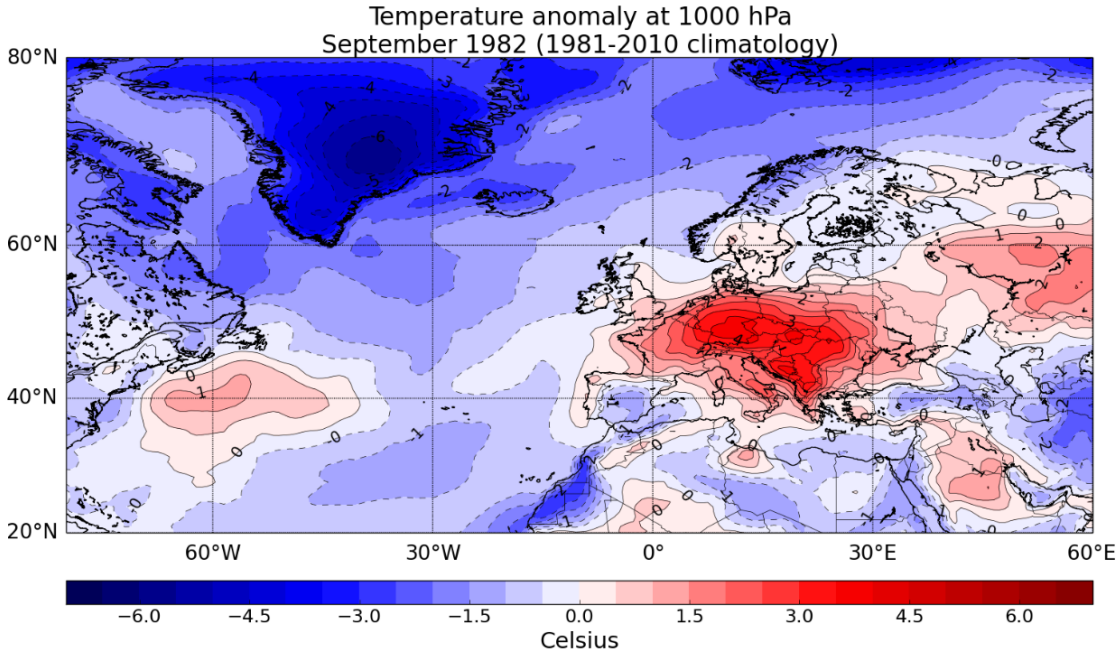

Figure 8. *Temperature anomaly (C) at 1000 hPa in September 1982 based on ERA-Interim reanalysis, with base period of September 1981-2010.*

A strong meridional tropospheric temperature gradient occurred over the North Atlantic and Scandinavia in September 1982 (not shown). It contributed the upper level winds to have abnormally high values in western and eastern parts of the North Atlantic; in these regions the upper level winds had strongly positive anomalies with magnitudes of 12-16 m/s (*Figure 9b*). Average upper level winds in September 1982 were the strongest in the western part of the North Atlantic reaching up to 40 m/s (*Figure 9a*). From *Figure 9a* can be seen that the mean jet stream occurred across the North Atlantic

and above the UK it curved to northeast. As discovered in the previous paragraph, the more northerly storm track, which is followed by the jet stream, is clearly seen from the *Figure 9b* as a positive upper level wind anomaly along the northerly track.

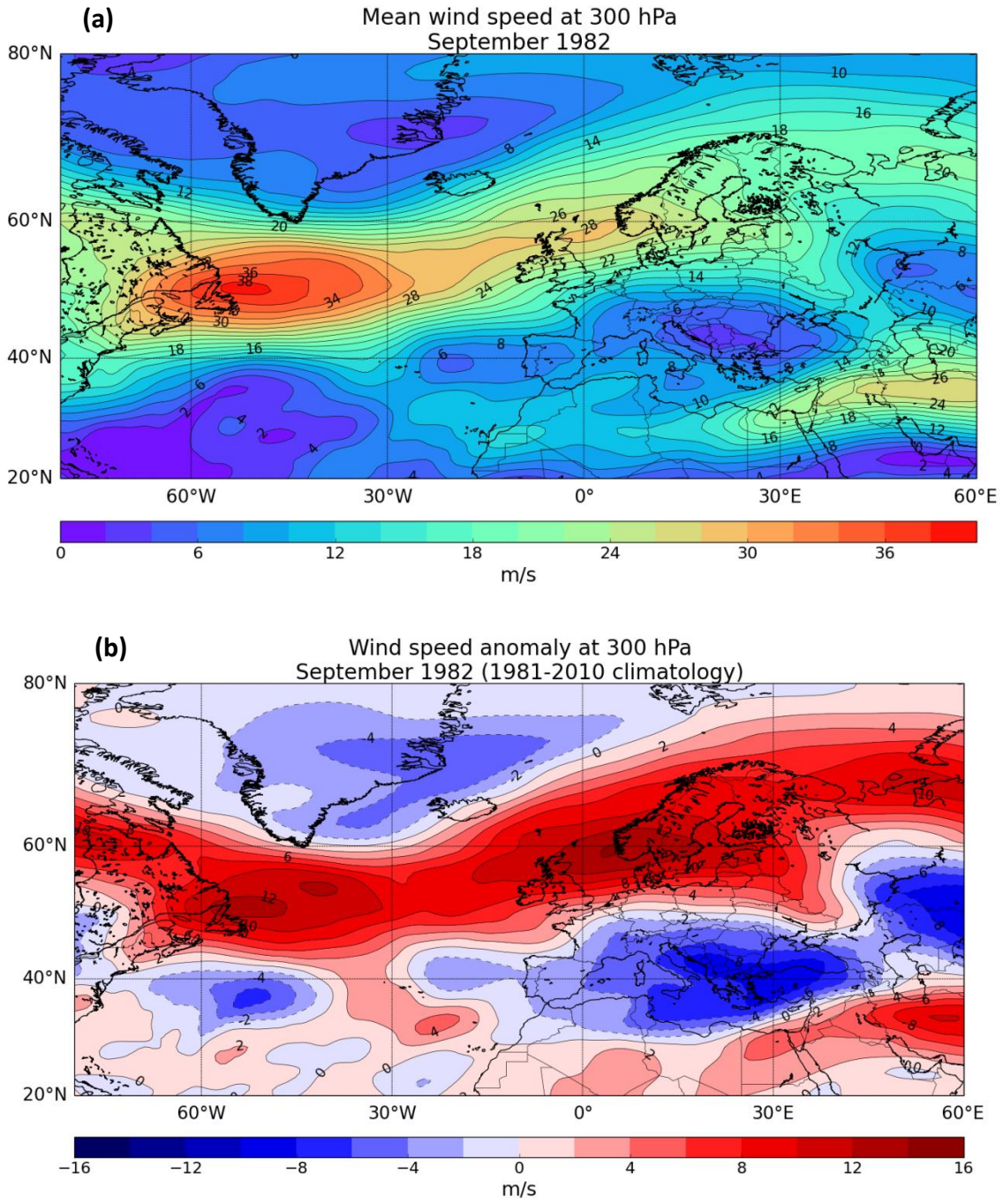

Figure 9. ***(a)*** *Mean 300 hPa wind speed (m/s) in September 1982, and* ***(b)*** *its anomaly (m/s, base period of September 1981-2010) based on ERA-Interim reanalysis.*

4.2. Development of hurricane Debby

Debby developed from an active tropical wave that moved to the north of the Caribbean; the only area in the Atlantic during September 1982 that had favourable atmospheric conditions, mainly low values of vertical wind shear, for tropical cyclone development (Clark, 1983). By the 13th of September a cyclonic circulation had formed along the ridge of the wave north of the Dominican Republic and the weak wind shear enabled it to intensify, thus being upgraded to a tropical cyclone named Debby on the morning of the 14th (*Figure 10*). Picked up by an approaching trough in the westerlies, Debby turned away from the US coastline moving slowly northward and late on the 14th it became a hurricane.

Figure 10. *The storm track of hurricane Debby every 6 hours from the 13th 12Z to the 20th 18Z September 1982. The colors indicate the stage of the cyclone: tropical depression (blue), tropical storm (green), hurricane categories 1-5 (yellow to pink) and extratropical cyclone (grey). Figure modified based on NOAA* (NOAA Historical Hurricane Tracks, 2016).

On the 15th the strengthening hurricane moved northeast towards Bermuda with an estimated minimum pressure of 966 hPa and surface winds of 48 m/s (Clark, 1983).

However, on the 16th Debby took a more northerly route and passed 130 km west of Bermuda with wind gusts near 30 m/s (Clark, 1983) causing only minor damage. Early on the 17th the forward speed of the hurricane decreased but already in the afternoon of that day it began to accelerate again due to an approaching trough in the westerlies. Debby reached its minimum pressure of 950 hPa by the night of the 17th with estimated maximum peak surface winds of 58 m/s (Clark, 1983) circa 750 km north of Bermuda and 750 km east of the US coastline. By the evening of the 18th the hurricane had passed southeast of Cape Race, Newfoundland, where wind gusts of 19 m/s and heavy rainfall were observed. Then Debby started to move rapidly eastward across the North Atlantic toward Europe meanwhile clearly weakening and over the ocean it transformed to an extratropical cyclone.

4.3. Storm track based on ERA-Interim and NOAA

The storm track of hurricane Debby and storm Mauri based on ERA-Interim is shown in *Figure 11*. According to that, Debby moved rather slowly alongside the east coast of North America. After passing Bermuda on the 16th, the hurricane travelled north and in the afternoon of the 17th, it sharply turned towards northeast. Keeping this direction Debby proceeded steadily and passed Newfoundland, Canada on the 19th between 00Z and 06Z. Then it started to curve eastward, was caught by the westerlies and due to that the speed accelerated. The cyclone moved rapidly across the North Atlantic in less than two days, passed the southwest coast of Ireland on the 21st 00Z and already reached the southern UK 6 hours from that. From there, the cyclone continued with the high speed and curved towards the northwest-east. On the same day at 18Z, the cyclone travelled over Denmark and after just few hours it landed to Sweden. The storm track stayed over land through the whole of Sweden. In the afternoon of the 22nd, the cyclone travelled across Lapland, Finland and got named storm Mauri. After finally reaching the Barents Sea on the 23rd, the storm turned eastward and started to decelerate.

The storm track of hurricane Debby by ERA-Interim reanalysis (*Figure 11*) can be compared to the same track by Historical hurricane tracks, NOAA (*Figure 10*). From the

comparison it can be seen that the locations of the low pressure centers are remarkably equal between these two tracks during the whole path of hurricane Debby. Both ERA-Interim and NOAA catch the sharp turn on the 17th, and when for instance examining the track past Newfoundland, the distances from the coastline and UTC times are exactly the same. Therefore, it can be shown that ERA-Interim tracked the cyclone evolution exceedingly well.

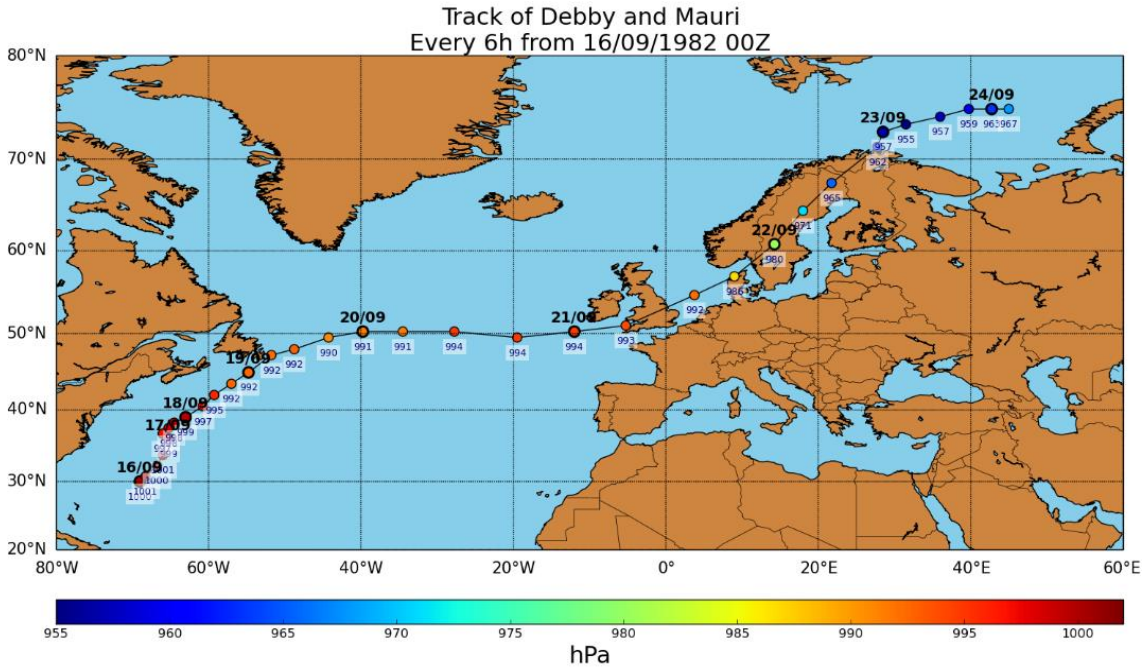

Figure 11. *The storm track (line) and intensity (colors, hPa) of Debby and Mauri every 6 hours from the 16th 00Z to the 24th 06Z September 1982. Days every 00Z are labelled.*

Based on NOAA, on the 16th 00Z, which is the starting time of the ERA-Interim storm track, the pressure was already 966 hPa (Clark, 1983). From the 16th to the afternoon of the 17th the pressure stayed stable, but in the next 12 hours it dropped 16 hPa and the hurricane reached its minimum pressure of 950 hPa. After that, Debby steadily started to lose its intensity. When the cyclone was over the central North Atlantic on the 20th the pressure had already risen to 996 hPa.

Compared to NOAA, in the ERA-Interim reanalysis the MSLP during the hurricane phase was significantly underestimated. Already in the beginning of the track on the 16th

00Z, the MSLP by ERA-Interim (1 000 hPa) was clearly higher than the pressure by NOAA (966 hPa). The quite stable pressure state by NOAA between the 16th and the 17th was seen by ERA-Interim as the MSLP varied only a few hPa at that time. However at night of the 17th, when Debby reached its minimum pressure based on NOAA, the value at the center of the hurricane by ERA-Interim was just 997 hPa. The deep pressure drop was not shown as strongly in ERA-Interim at any moment during the Debby phase; after the 17th the MSLP first fell 5 hPa in the next 12 hours starting from the value 997 hPa and then stayed at 992 hPa all the way from the 18th 12Z to the 19th 12Z. Now Debby had passed Newfoundland and was rapidly moving across the North Atlantic. Based on ERA-Interim, the MSLP slightly weakened over the ocean and held the 994 hPa pressure until the remnant of Debby reached the UK. At this point the pressure differences between ERA-Interim and NOAA had faded out.

After passing the UK on the 21st 12Z, the cyclone began the rapid deepening (*Figure 11*). During the next day the MSLP had decreased from 992 hPa to 965 hPa which is a major pressure drop of 27 hPa in 24 hours. Taking the effect of latitude into account, the 24 hour pressure fall of 24,3-27 hPa was calculated starting from the 21st 12Z to the 22nd 00Z. Hence, the storm was classified as a meteorological bomb. The intensifying maintained while the cyclone moved over Sweden and Lapland, and the lowest pressure of 955 hPa occurred when Mauri just reached the Barents Sea. After that, the cyclone decelerated and the intensity started to gradually decay.

One reason for the underestimation of the pressure values by ERA-Interim is that it is a reanalysis whereas the storm track by NOAA is a combination of a reanalysis and observations from several organizations. In addition, the number and quality of observations for the ERA-Interim reanalysis has increased greatly from the 1980's to the 21st century; for example the number of different instruments for the radiance data was only 6 in 1989 and nearly 20 in 2010 (Dee, et al., 2011). Also, the resolution of the dataset has a major impact on the pressure values of a cyclone since too low resolution does not find a cyclone as intense as a higher resolution does. Further thoughts on the accuracy of the ERA-Interim storm track are discussed in *section 5*.

4.4. Extratropical transition

4.4.1 Extratropical transition onset

For this thesis the B–index is calculated every 6 hours from the 16th 00Z to the 24th 00Z of September 1982, and the results, time series of the B–index evolution, are shown in *Figure 12*. Debby stayed symmetric when it travelled past Bermuda on the 16th and reached the highest intensity on the 17th. It can be seen that Debby started ET already on that day at 18Z, when the B–index reached the value of +12,6. After that, the B–index increased slowly and steadily as the cyclone moved northward alongside the east coast of America. Thus, the cyclone was gradually losing its eye structure. On the 19th 12Z there was suddenly a giant stride in the B–index towards higher values. *Figure 11* shows that at the same time the now transitioning cyclone started its path across the North Atlantic and accelerated due to westerlies. Moving over to the mid-latitude environment, the increasing baroclinicity and vertical wind shear made the structure to stretch and quickly change form into clearer fronts. The highest B–index values, meaning the most front-like structure, occurred between the 20th 12Z and the 21st 06Z when the cyclone swept over the ocean and at the end arrived to the coast of the UK. This was also the time period when the MSLP was quite stabilised.

Following the frontal phase, a sudden drop in the B–index values began and the decrease proceeded steeply. At the same time the cyclone reached the blocking high pressure area over central Europe and turned towards northeast. The rapid decreasing of the B–index values continued while the storm moved across Sweden and Lapland, and was then named Mauri. The B–index decreased to values less than 10 again at the night of the 22nd, and at the 23rd 00Z the B–index was already decreased to -19,6 which was the lowest value during the evolution of both the hurricane Debby and storm Mauri. Decreasing below the threshold value of 10 means that the cyclone was once again defined as symmetrical indicating barotropic structure. Symmetricity is typical for an occlusion. At that time Mauri had just passed Lapland and reached the Barents Sea. Right after the minimum peak in the B–index, the values balanced back towards the value +10. Meanwhile, the storm had finally decelerated over the cold sea.

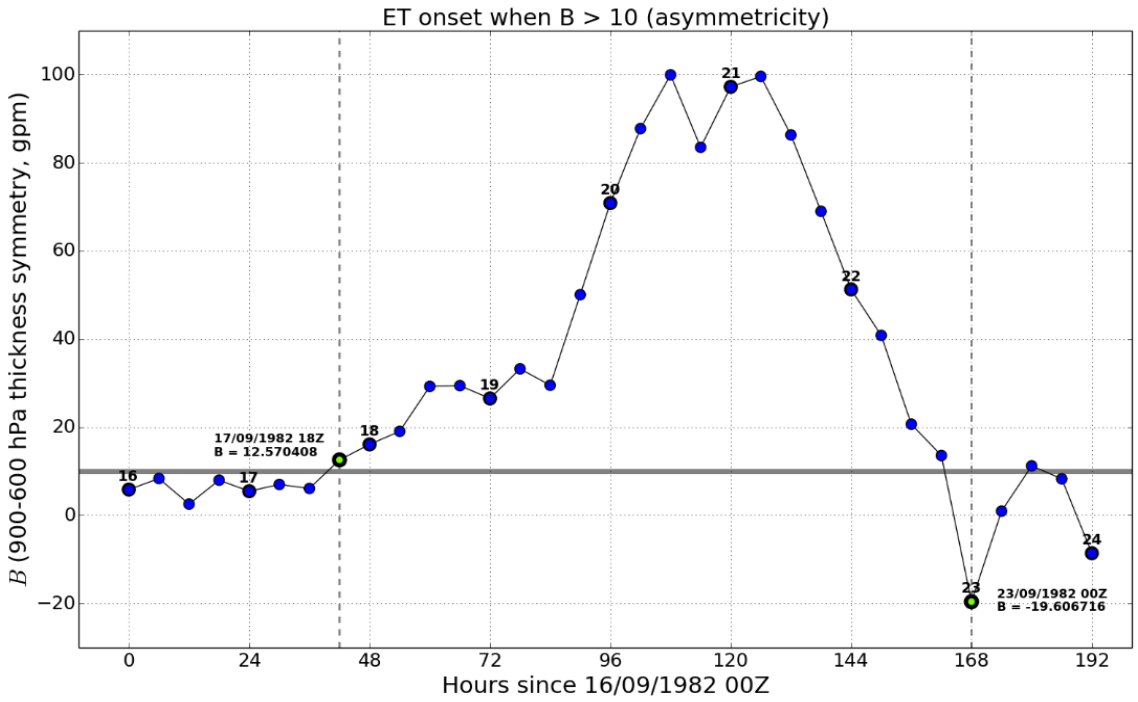

Figure 12. *B-index (900-600 hPa thickness symmetry) every 6 hours from the 16th 00Z to the 24th 00Z of September 1982. The first green circle is the time when B value gets greater than 10 meaning ET onset and the latter circle signifies the time when B reaches values below 10 again. Numbers above circles are dates of September every 00Z.*

4.4.2 Extratropical transition completion

The calculated thermal wind (from now on the V_T –index) is computed from the 16th 00Z to the 24th 00Z of September 1982, and the results of the V_T –index calculations are shown in *Figure 13*. The V_T –index decreased steadily with minor fluctuations all the way from the 16th 00Z (*Figure 13*), when Debby travelled alongside the east coast of America, to the 21st 12Z, when the cyclone had just passed the UK. The thermal wind difference turned slightly negative for the first time on the 18th 06Z but bounced back to positive shortly after that. SSTs under Debby decreased while the storm was moving more north, and that made the latent heat release, which is the main energy source for a tropical cyclone, to decrease. Due to the growing influence of the mid-latitude environment, the vertical wind shear increased cutting off the vertically aligned heating, which causes the air to rise high. Properly the negative phase began on the 19th 06Z with the V_T –index value of -27,6. That was just after Debby had passed Newfoundland and

was starting the rapid crossing over the North Atlantic. ET had started on the 17th 18Z by turning asymmetrical (see *section 4.4.1*). On the 19th 06Z, when the warm core has changed to a cold one, the ET was finally completed. Thus, Debby had transformed to an extratropical cyclone.

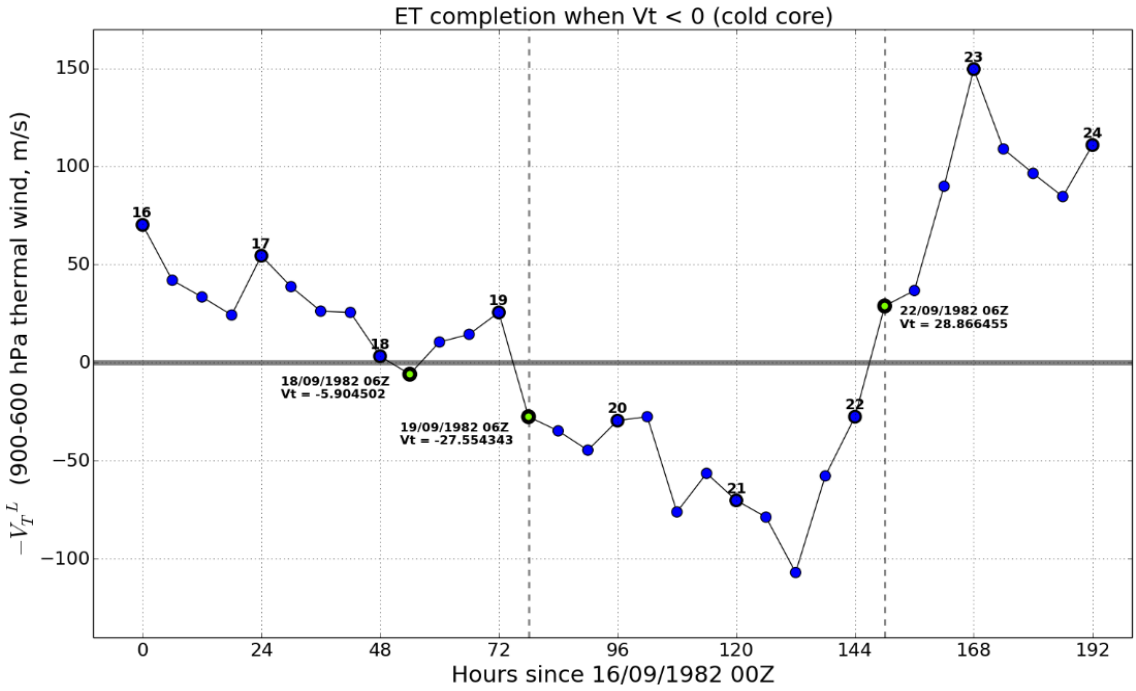

Figure 13. *V_T-index (900-600 hPa thermal wind) every 6 hours from the 16th 00Z to the 24th 00Z September 1982. The first green circle is the time when V_T value goes under 0 the first time but only shortly, and the second green circle is the time when V_T value turns negative and ET is entirely completed. The latter circle signifies the time when V_T reaches positive values again. Numbers above circles are dates of September every 00Z.*

On the 21st 12Z there was a sudden change in the direction of the V_T –index as the decreasing trend turned to increase. At that time the transformed extratropical cyclone had already passed the UK and began to curve towards Scandinavia. Also the B–index trend had turned from increase to decrease just 6 hours before. The increase of the V_T –index continued steeply reaching positive values again in less than 18 hours. On the 22nd 06Z the V_T –index was already +28,8 and the highest value of the V_T –index occurred on the 23rd 00Z. That is the same time when the B–index had its lowest value. After that the V_T –index trend turned back to decrease towards a cold cored structure.

4.4.3 Phase diagram

For Debby and Mauri case the parameters needed in a phase diagram are calculated in previous *sections 4.4.1* and *4.4.2* and the phase diagram is plotted in *Figure 14*. As a hurricane, Debby had a symmetric and warm core structure and the tropical phase of the cyclone can be seen in the bottom right panel of the phase diagram. The ET onset occurred in the 17th 18Z while the tropical cyclone was moving along eastern America. Next 30 hours Debby stayed warm cored but since moving to the cooler SSTs toward higher latitudes it completed ET on the 19th 06Z. Therefore, the transitioning took 36 hours. The mean duration of ET is 33,4 hours (Evans & Hart, 2003) so Debby's transition time was quite average.

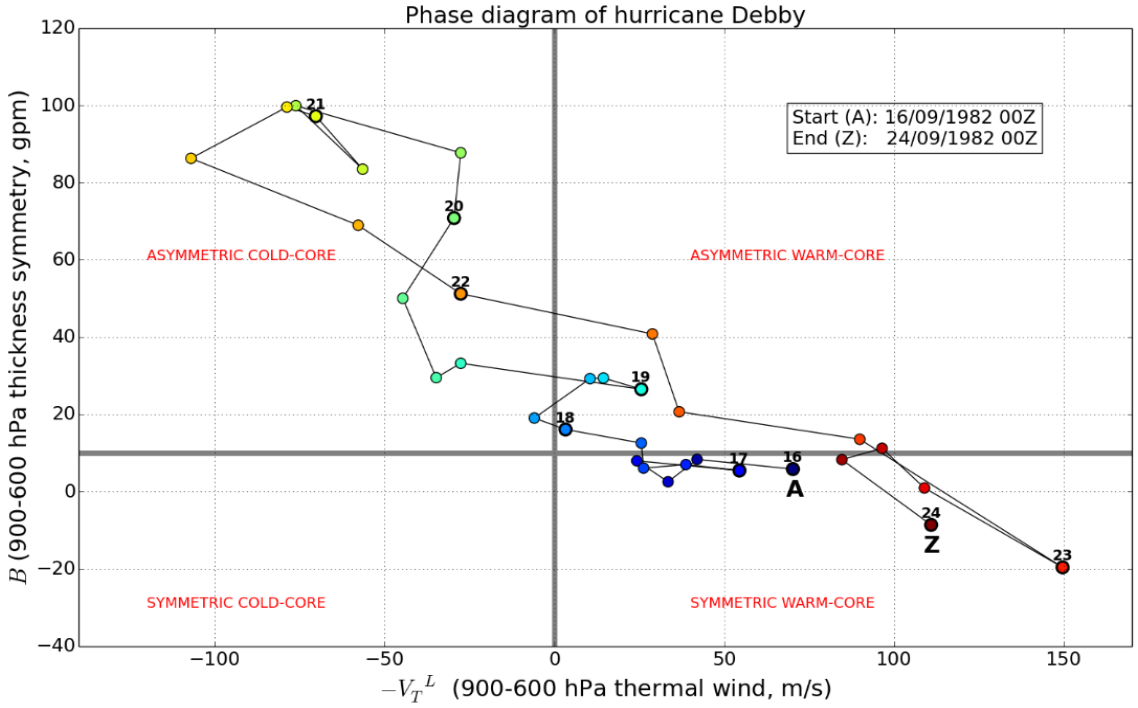

Figure 14. *Cyclone phase diagram as presented in Hart (2003) every 6 hours from the 16th 00Z to the 24th 00Z September 1982. The x-axis (-V_T, thermal wind, m/s) indicates whether the cyclone is cold or warm cored and the y-axis (B, thickness symmetry, gpm) indicates whether the structure of the cyclone is symmetric and non-frontal or asymmetric and frontal. Letter A refers to the starting time (16th 00Z) and Z to the ending time (24th 00Z). Marker colors change during time. Numbers above the circles are 00Z times of September.*

The extratropical phase is shown in the top left panel in *Figure 14* with asymmetric and cold core structure. The now transformed cyclone strengthened its extratropical features until the 21st 12Z when it had just passed the UK. Then the cyclone started rapidly to lose these features and regained the warm core structure in less than 18 hours. At that time the cyclone was already over central Sweden. Continuing the fast transitioning the storm, now named Mauri, swept over Lapland on the 22nd 12Z-18Z. Right after that, Mauri finally regained the symmetric features. Having turned warm cored already before, now the whole structure of the storm was similar to a tropical cyclone. That was due to the occlusion which will be shown in *section 4.6*. As seen in *Figure 14*, the tropical characteristics are clearly more intense with Mauri over the Barents Sea than in the beginning with hurricane Debby. *Section 4.6* presents a more detailed review about the synoptic conditions that affected to the development and intensity of storm Mauri.

4.5. Vertical PV distribution

For a tropical cyclone, the vertical PV distribution is typically dominated by the diabatic tower feature and it is not influenced by the stratosphere (Lackmann, 2012). In *Figure 15a*, a vertical cross section of PV is presented at the 17th 06Z when Debby was still a hurricane. The characteristic PV tower of a tropical cyclone can be clearly seen, and there is high PV in the stratosphere. PV anomalies in the troposphere do not appear to have stratospheric origins. Hence, PV distribution in the hurricane Debby phase had diabatic origin, as typical for a tropical cyclone. PV maxima were located between 600-500 hPa pressure levels and, on a smaller area, between 1000-900 hPa pressure levels. Both PV maxima were situated vertically above the surface low pressure center.

When a tropical cyclone moves towards higher latitudes and begins extratropical transition, the vertical PV distribution starts to change (Lackmann, 2012). The dynamic tropopause (i.e. the 2 PVU surface) penetrates towards the troposphere and the stratospheric PV begins to impact the PV distribution. At the same time, the diabatic PV tower at the lower troposphere retains its structure. Hence, there are two clear PV maxima both in the stratosphere and in the lower troposphere, and at this stage these

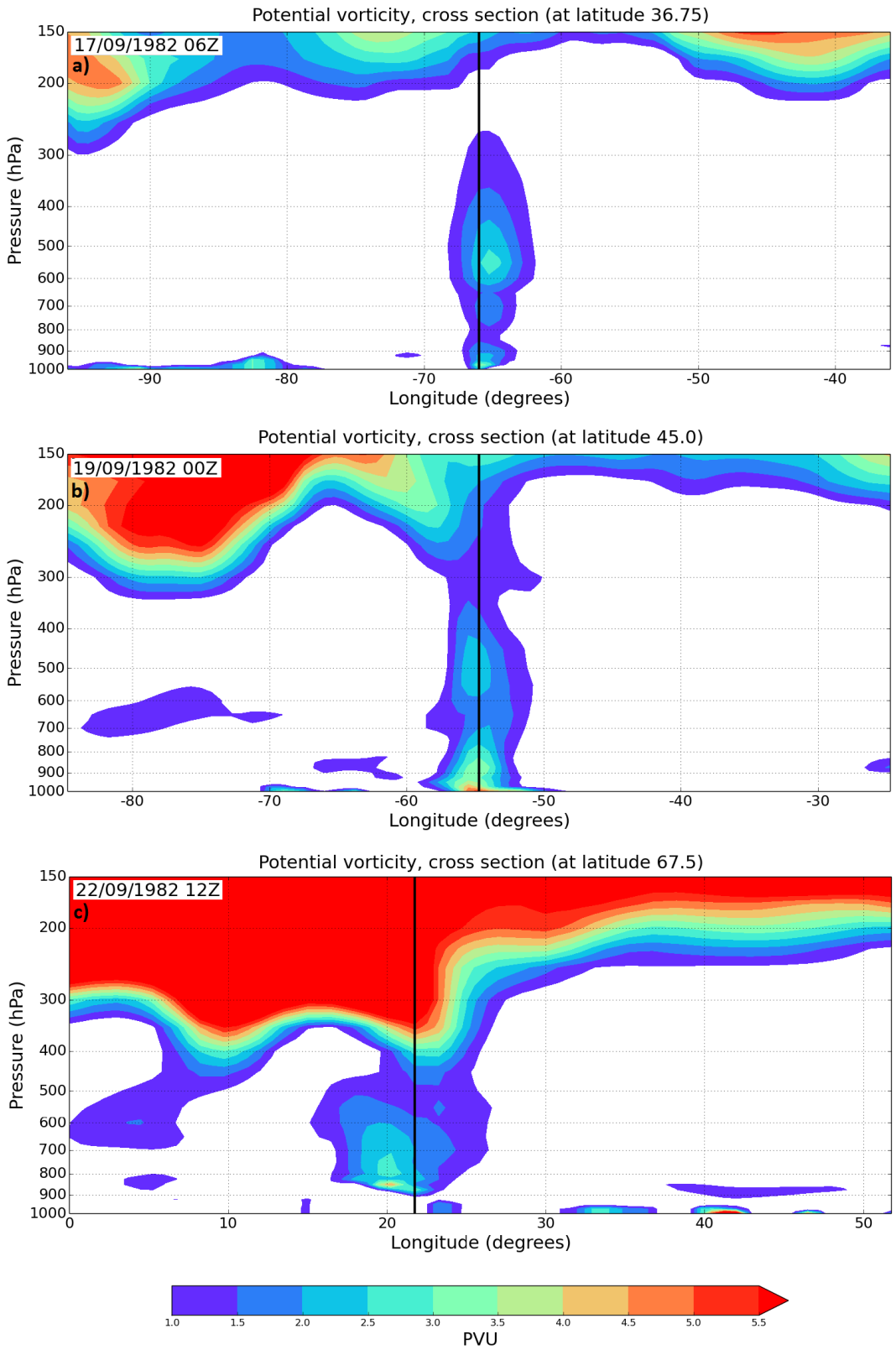

Figure 15. *Cross sections of potential vorticity (PVU)* ***(a)*** *17th 06Z,* ***(b)*** *19th 00Z, and* ***(c)*** *22nd 12Z in September 1982. Cross sections are calculated along the latitudes (degrees written in the titles). The black line indicates the longitude where the low pressure center locates.*

are usually still distinctly separated. In the case of Debby, the stratospheric PV penetrating towards the lower troposphere can be seen when the cyclone was undergoing ET (*Figure 15b*). Despite of the strengthening upper level PV, the PV tower was distinct in the lower levels. The PV maximum locating between 600-500 hPa pressure levels was still visible but it had slightly weakened. However, the PV maximum near the surface had clearly strengthened and the surface area of the higher PV values had doubled its width.

For an extratropical cyclone, the vertical PV distribution is originated strongly from the stratosphere and is just partly contributed by the diabatic processes from the lower troposphere (Lackmann, 2012). There is stronger stratospheric PV in polar regions and the dynamic tropopause is at lower levels than in tropics. Typically, the vertical PV distribution associated with an extratropical cyclone is not isolated from the stratospheric PV, and the highest values are in the upper levels with a peak towards the low pressure center. *Figure 15c* is plotted at the time the cyclone was reaching Lapland (and named Mauri) and had just turned back to a warm cored cyclone. The location at the higher latitudes is clearly seen as strong stratospheric PV and lower tropopause, and the peak downwards above the surface low pressure center can be noted (*Figure 15c*). However in the Mauri phase, unlike in the typical extratropical cyclone structure, the diabatic lower level PV feature was distinctly separated from the stratosphere. The maximum PV at the lower levels had isolated from the surface and risen to the 900-800 hPa pressure levels. The horizontal structure of the tower had greatly broaden but vertically the height of the tower had decreased. The lower level PV was probably due to diabatic heating in the warm sector which will be shown in next *section 4.6*.

4.6. Development of storm Mauri

Over the North Atlantic the location of ex-Debby, the already transformed extratropical cyclone of original hurricane Debby, was right behind an upper level trough downstream of a ridge axis (not shown) which is a region where NVA occurs. NVA implies to convergence at upper levels that is associated with subsidence and therefore that is a non-favourable area for the development of a cyclone. That made ex-Debby to weaken

as shown in *section 4.3*. However, the strong jet stream across the North Atlantic made the cyclone move rapidly towards Eastern Europe. The storm was now situated on the right side of jet entrance (not shown) which indicates ascent and thus enhances cyclogenesis. As a result, the weakening of the cyclone due to the placement behind the upper level trough downstream of the ridge was reduced by its favourable location in the strong jet stream.

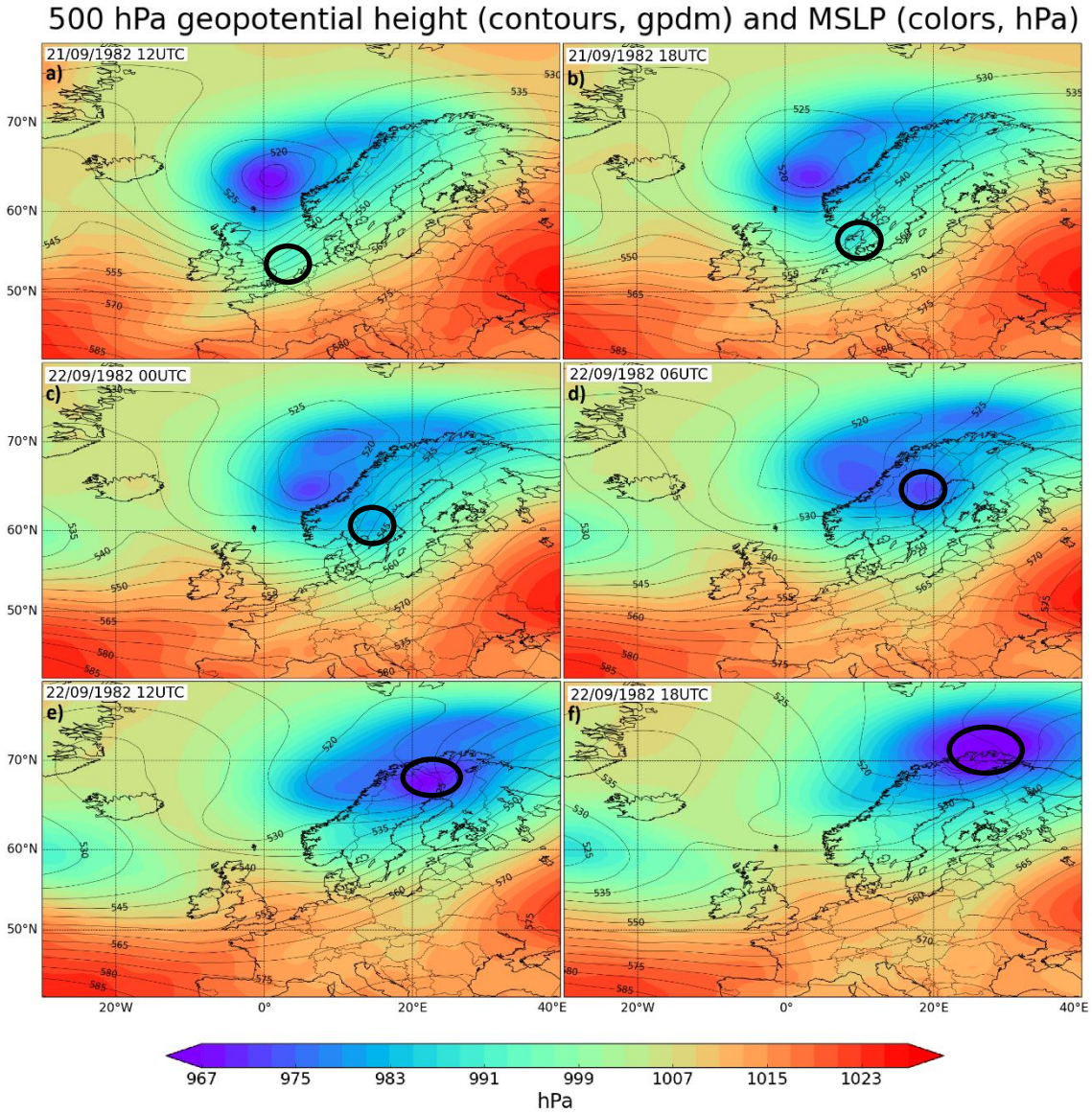

Figure 16. *Geopotential height at 500 hPa (contours, gpdm) and mean sea level pressure (colors, hPa)* ***(a)*** *21st 12Z,* ***(b)*** *21st 18Z,* ***(c)*** *22nd 00Z,* ***(d)*** *22nd 06Z,* ***(e)*** *22nd 12Z, and* ***(f)*** *22nd 18Z in September 1982. The circle shows the location of ex-Debby and Mauri cyclone.*

After the speedy transit across the ocean, the cyclone had quickly passed the UK in the morning of the 21st. Because of the rapid proceeding, ex-Debby finally caught up the upper level trough (*Figure 16a & b*). Accordingly, the storm was then moving towards a PVA region away from the subsidence created by NVA. That started to strengthen the cyclone. At the same time, the location of ex-Debby remained on the right side of jet entrance (*Figure 17a & b*) as the strong jet stream turned towards Scandinavia, followed by the cyclone.

Due to the strong high pressure area over central Europe (*Figure 8*), a warm southerly flow dominated over Finland and there was a large warm air mass above these regions. On the contrary, a clearly cooler air mass occurred over the Norwegian Sea. These two air masses formed a long meridionally oriented cold front between them. A zonally oriented warm front occurred next to the coastal area in the Barents Sea reaching towards east, and the cold and warm fronts met perpendicularly beside the seaside near the northernmost Lapland. From this region, an occluded front extended westward alongside the coast curving south over the Norwegian Sea. Just off the east coast of Norway there was a strong low pressure center associated with the occluded front (from now on referred to as the 2nd cyclone). This 2nd extratropical storm was highly equal to the Shapiro-Keyser model cyclone with the T-bone structure and bent-back front. The frontal structure of the 2nd cyclone was also found in the hand-drawn synoptic maps from the microfilms made in 1982.

In the early morning of the 22nd, ex-Debby had finally proceeded right ahead of the trough (*Figure 16c & d*), which is where PVA is at its most intense, and the cyclone had already significantly strengthened. The low pressure center with respect to the still strong jet stream stayed on the right side of jet entrance (*Figure 17c & d*) as both the cyclone and the jet stream moved at the same speed across Sweden. Strengthening ex-Debby interacted with the pre-existing long cold front and caused a wave disturbance along the front (*Figure 18a*) meanwhile the 2nd low pressure center stayed over the Norwegian Sea and slowly started to weaken.

On the 22nd 12Z, the jet stream started to weaken and shift eastward across Finland (*Figure 17e*), meanwhile ex-Debby hit Lapland and was named storm Mauri. Also,

the upper level trough began to weaken but in spite of that, the cyclone retained its favourable location right ahead of the trough (*Figure 16e*). At the same time, the 2nd cyclone merged with Mauri making the storm even more intense. The cyclone had now developed the wave disturbance into a proper frontal structure in the middle of the pre-existing cold front (*Figure 18b*). The occluded bent-back front started to approach Mauri bringing warmer air around the low pressure center.

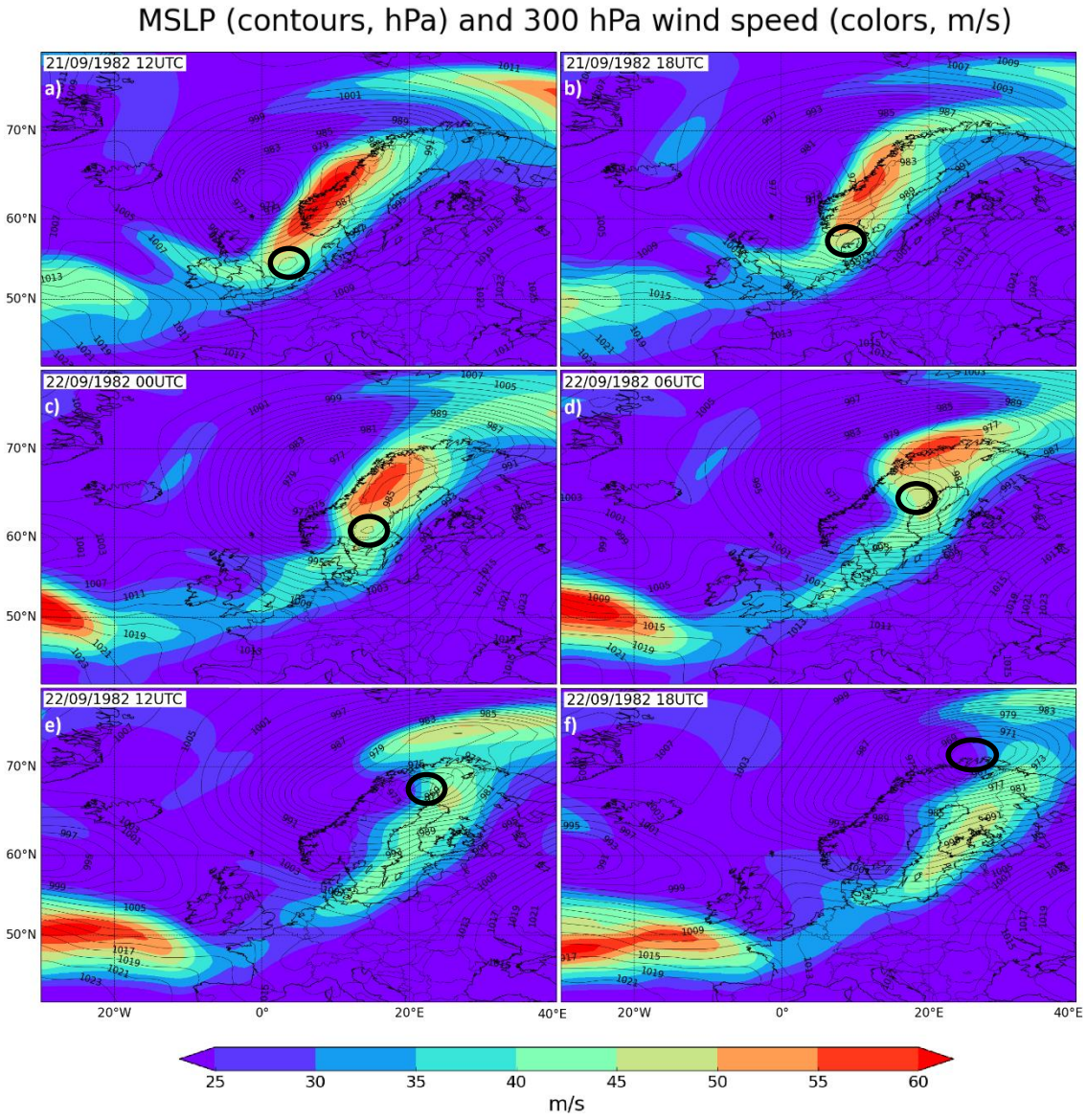

Figure 17. *Mean sea level pressure (contours, hPa) and wind speed at 300 hPa (colors, m/s)* ***(a)*** *21st 12Z,* ***(b)*** *21st 18Z,* ***(c)*** *22nd 00Z,* ***(d)*** *22nd 06Z,* ***(e)*** *22nd 12Z, and* ***(f)*** *22nd 18Z in September 1982. The circle shows the location of ex-Debby and Mauri cyclone.*

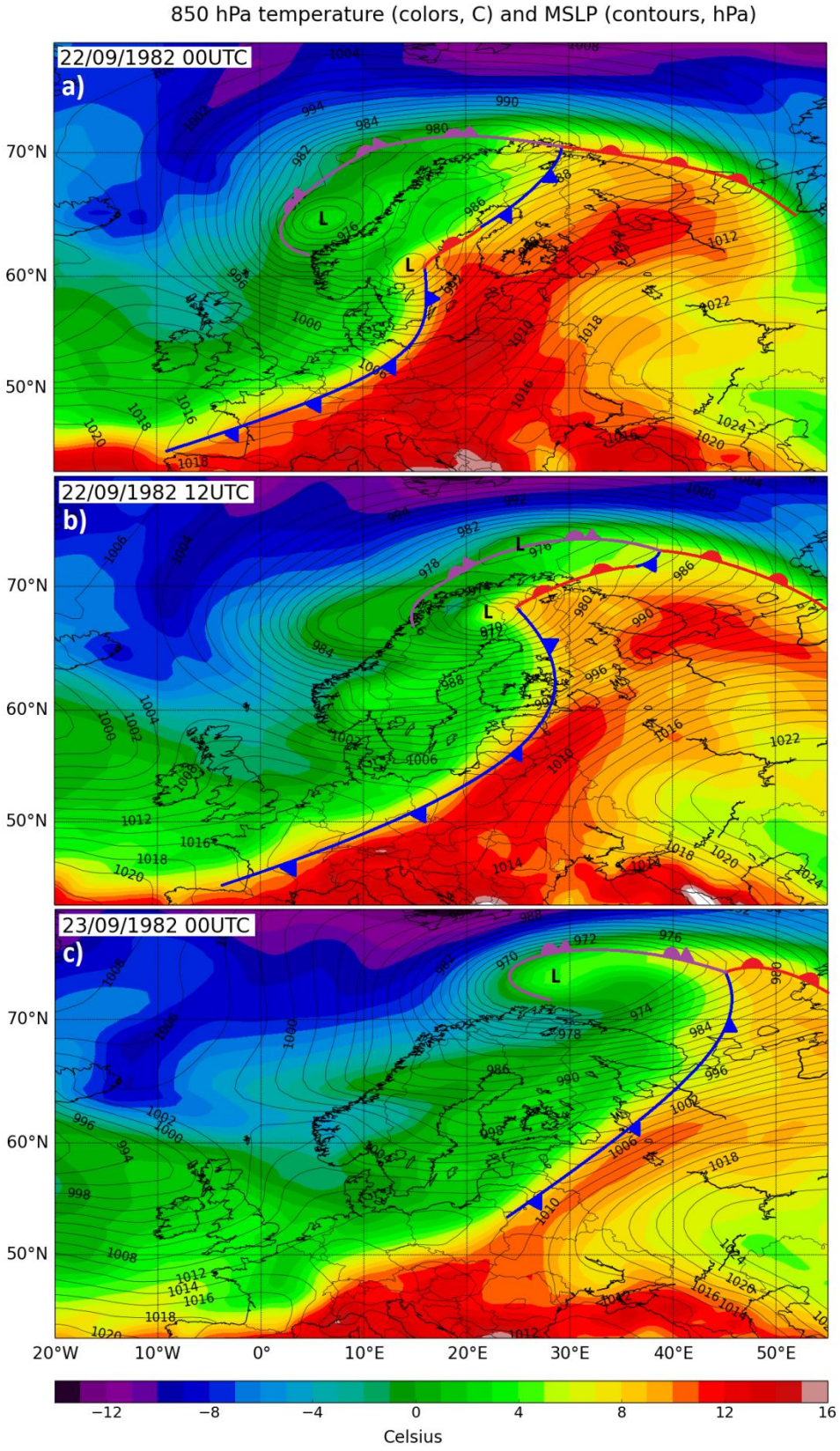

Figure 18. *Temperature at 850 hPa (colors, °C), mean sea level pressure (contours, hPa) and fronts* ***(a)*** *22nd 00Z,* ***(b)*** *22nd 12Z, and* ***(c)*** *23rd 00Z in September 1982.*

It is known that when the surface low pressure center gets warmer than the surrounding air, usually due to an occlusion and/or a warm seclusion, an extratropical cyclone can also have a warm core (Wallace & Hobbs, 2006). The occluded front, that approached Mauri, gathered warm air to the low levels over the surface low pressure center. Hence, the cyclone turned back to a warm cored system. The strongest winds observed by FMI were 30 m/s (10 min average wind) on the 22nd 12Z (3 pm local time in Finland). That was measured in Ajos weather station which is situated in a cape at the open sea in the Bothnian Bay. Therefore, the storm did not quite reach the hurricane force winds of exceeding 32 m/s. In land, the strongest 10 min average winds of 22 m/s were measured in Pokka, Northern Lapland on the 22nd 18Z. To comparison, ERA-Interim did not reach to that high values; based on the reanalysis the strongest winds were only 17 m/s locating in the Bothnian Bay. It can be clearly stated that the values by the reanalysis are significantly underestimated.

After the storm had swept forcefully over Lapland, it was caught up by the upper level trough (*Figure 16f*) while still being extremely intense. At that time, the poleward oriented cold front weakened meanwhile the occluded bent-back front had backtracked towards the Barents Sea and it wrapped the low pressure center around it (*Figure 18c*). Warmer air was trapped inside the storm center and the occluded front formed a warm seclusion. This enhanced the warming of the core. Moreover, the wrapping of the occluded front together with the warm seclusion made the cyclone lose its frontal structure on the 23rd 00Z and turned it back to being symmetric. Then the storm continued its path towards the open sea and over time slowly started to weaken.

4.7. Comparison to other storms

In this section, two other storms, hurricane Maria from 2005 and winter storm Kyrill from 2007, will be compared with Mauri. The case of hurricane Maria is chosen because its life cycle was similar to Mauri; it completed ET, travelled to Europe and re-intensified (Beven II, et al., 2008). Kyrill was not a hurricane but an extremely intense storm that caused major damage in central Europe (Fink, et al., 2009). Like Mauri, Kyrill became a meteorological bomb that developed over the North Atlantic and re-

intensified over European continent due to a favourable positioning of polar jet streaks and dry air intrusion. Therefore, Mauri can be compared to a storm that also originated from a hurricane and underwent extratropical transition and additionally to a storm that developed to a meteorological bomb and re-intensified over land. Hence, Mauri is in a way a combination of the features from Maria and Kyrill.

Table 2. *Comparison between storms Mauri, Maria and Kyrill. Sources of information: Debby/Mauri: ERA-Interim results, FMI reports, Maria: Beven II, et al. (2008), Bergens Tidende (2006), National Hurricane Center - Discussion reports, Kyrill: Fink, et al. (2009), Swiss Re Group (2008), Indices: NOAA. (SON = Sept-Nov, ASO = Aug-Oct, JFM = Jan-Mar, EC = Extratropical Cyclone)*

	Debby / Mauri	**Maria**	**Kyrill**
Date	13th - 22nd Sept 1982 (20th → EC)	1st – 14th Sept 2005 (10th → EC)	15th – 24th Jan 2007
Duration	10 days (7 TC + 3 EC)	14 days (9 TC + 5 EC)	10 days
Origin	Hurricane (Category 4)	Hurricane (Category 3)	Extratropical cyclone
Min. pressure	950 hPa (Debby) ~964 hPa (over Finland) 955 hPa (over Barents Sea)	962 hPa (as hurricane) 962 hPa (as EC)	962 hPa
Max. wind	58 m/s (1min, Debby) 22 m/s (10min, land, Pokka) 30 m/s (10min, sea, Ajos)	51 m/s (1min, as hurricane) 30 m/s (10min, land as EC)	> 33 m/s (10min) > 56 m/s (gust, mountain top) 40 m/s (gust, lowland)
ENSO-index	+1,70 (SON, very strong El Niño)	+0,02 (ASO, towards La Niña)	+0,32 (JFM, weakening El Niño)
NAO-index	+1,76 (strongly positive)	+0,63 (positive)	+0,22 (weakly positive)
AO-index	+0,558 (positive)	+0,802 (positive)	+2,034 (strongly positive)
Impacts	2 fatalities (EC) 30-50 million EUR economic loss	3 fatalities (EC) 3 million EUR economic loss	at least 46 fatalities 5 billion EUR economic loss
Meteorological Factors	1) Re-intensified over land 2) Merged with another EC 3) Warm seclusion 4) Tropical structure	1) Re-intensified over sea 2) Merged with another EC 3) Hurricane-force winds over sea as EC	1) Re-intensified over land 2) Dry air intrusion 3) Alignment of three polar jet streaks

The main characteristics of the storms have been collected to *Table 2*. It can be seen that all three of the storms had a really long lifetime of 10-14 days. The minimum pressure values were also quite comparable between them. Kyrill had the strongest winds as an extratropical cyclone, over 33 m/s, reaching to hurricane force speeds. Nevertheless, the maximum winds associated with Mauri and Maria were not that far

(30 m/s). The climatological conditions based on NAO- and AO-indices were similar as in all cases both indices were positive.

Comparing the impacts, Mauri and Maria hit most badly only one country causing few fatalities (Mauri in Finland, Maria in Norway). Still, the economic loss was over ten times higher with Mauri (see *Table 2*). Kyrill, however, swept over a wide region in central Europe and claimed at least 46 fatalities and made even hundred times worse economic loss than Mauri (see *Table 2*). By looking at the ENSO-index, it can be noticed that even though they all had positive values they were still in very different phases (strong, weak or near zero). ENSO phase has an impact mostly to the tropical cyclone frequency but it also affects to extratropical cyclones changing the normal storm tracks and causing temperature and precipitation anomalies in many regions (NOAA Warm Episodes, 2012). Strong El Niño occurred from these cases only during Mauri and it might have had an impact on the anomalies over Europe in 1982.

5. DISCUSSION

The findings of this thesis suggest that storm Mauri was the remnant of hurricane Debby. The results from ERA-Interim reanalysis show a precise storm track which begins from hurricane Debby alongside the east coast of North America, proceeds across the North Atlantic and ends up passing Scandinavia and Lapland as storm Mauri. Debby was associated with a warm core and symmetric structure, as typical for a tropical cyclone, and these features turned to a cold core and asymmetric fronts during extratropical transition. However, the results indicate that when crossing Sweden, the cyclone became warm cored again, and right after Mauri passed Lapland, it became symmetrical too.

Even though the transitioned cyclone ex-Debby weakened while crossing the North Atlantic, due to its favourable location for cyclogenesis on the right side of jet entrance, it did not decay. Positive surface pressure and temperature anomalies over central Europe made the strong jet stream, followed by ex-Debby, to shift northward

after passing the UK, and the cyclone re-intensified. Also, positive NAO and AO indices caused the storm track in general to move more north. Hence, climatic conditions favoured the cyclone to travel to higher latitudes. Over Sweden, ex-Debby proceeded right ahead of an upper level trough, a favourable position for cyclogenesis, and that made the cyclone to rapidly deepen up to 27 hPa in 24 hours defining the storm as a meteorological bomb. There was another strong extratropical cyclone over Scandinavia, and its low pressure center above the Norwegian Sea was merged with Mauri over Lapland. The occluded bent-back front wrapped Mauri around it trapping warmer air inside the storm center and a warm seclusion formed. The results suggest that it was due to the occlusion and warm seclusion that the structure of the cyclone changed back to warm cored and symmetric.

The storm track by ERA-Interim shows a consistent link between Debby and Mauri. However, because of merging with the pre-existing extratropical cyclone above the Norwegian Sea, it is harder to confirm that storm Mauri was developed only due to the remnants of Debby. Nevertheless, the results show that ex-Debby intensified before coming to the vicinity of the other cyclone, and its direction towards Lapland did not change even after merging. This indicates that the other cyclone was probably absorbed by Mauri and not the other way around. Additionally, the low pressure center of the other cyclone stayed over the Norwegian Sea but after merging with ex-Debby, the merged cyclone took ex-Debby's track northward. Hence, the track of the other cyclone would possibly have not passed Lapland without ex-Debby changing its direction. All these features support the proposition that Mauri would have not occurred without Debby.

Grams et al. (2011) examined a case of hurricane Hanna that underwent extratropical transition in September 2008. A Mediterranean cyclone Olivia occurred one week later, and they wanted to confirm the linkage between these two storms. That was investigated by using a methodology where the positive PV anomaly associated with the tropical storm was removed right before its interaction with the mid-latitude jet stream. The model was run with both the original analysis and with the modified analysis without Hanna. The difference between these model-runs showed the effects of the tropical

cyclone, and it enabled to determine the impacts of Hanna on the mid-latitude flow and on the development of Olivia. For further research in the case of hurricane Debby and storm Mauri, the same methodology could be applied as in Grams et al. (2011). In that way, it could be investigated how strong the impact of ex-Debby was on the development of Mauri. Hence, it could be confirmed whether hurricane Debby really was the main cause of storm Mauri.

The results show that ERA-Interim successfully found the correct locations for the storm track and vertical and horizontal structures of the cyclone, even though underestimating the intensity of the storm. ERA-Interim is purely a reanalysis in contrast to the storm track by NOAA, which is a comparison of a reanalysis and, most importantly, observations from many different agencies. Supposedly, ERA-Interim has some uncertainties in the sea level data over coastal America at the time period of Debby so that it does not catch the most intense values for the surface parameters. It is noted (Dee & NCAR Staff, 2016), that understanding and quantifying uncertainties in the ERA-Interim data is difficult. Mostly the limitations of the data are due to shortcomings in the assimilating model or methodology, lack or errors in observations or lack of information about errors. However, progress have been made and ERA-Interim has improved on for instance low-frequency variability and analysis accuracy. Regardless of not finding surface parameters intense enough, the correct low pressure center locations and structure features indicate that ERA-Interim is successful of tracking and calculating the cyclone evolution and characteristics.

The ERA-Interim reanalysis produces output in 6-hour intervals. With more frequent time step intervals, the timing of a specific event and values of quantities would become more accurate. For instance, more exact location, timing and intensity of the highest wind speed and the lowest surface pressure associated with storm Mauri could be achieved. Also, the synoptic evolution could be analysed more detailed which further would clarify the merging of ex-Debby and the other cyclone. Mauri swept rapidly over Finland in less than 6 hours and unfortunately there was no dataset available at the time the low pressure center of Mauri occurred over Lapland. Hence, more detailed study of storm Mauri could be analysed with more frequent time intervals.

In order to investigate the capabilities and weaknesses of using a certain reanalysis data, it would be important to compare the ERA-Interim results of this thesis with other reanalyses. Varying qualities, i.e. the resolution, could be compared among different reanalyses. Moreover, the results could be examined with not only other reanalyses but with weather prediction models and climate models. Weather prediction models are based on primitive equations, they aim to forecast the weather typically for around 10 days, and the details and times are more important (NCAR Analyzed and Model Data, 2016). Climate models are made for longer time periods, tens or hundreds of years, they are more focused on the statistics, and the resolution is usually lower. Thus, comparison between other types of models could bring forth strengths and weaknesses of using a specific model type.

It is not yet known how climate change will affect tropical and extratropical cyclones, their characteristics and extratropical transition. However, it is already been shown (Haarsma, et al., 2013) that when SSTs increase, the region in the Atlantic basin for hurricanes to develop will extend eastward and therefore more storms will continue their travel curving towards Europe. Thus, when climate change increases SSTs also the origin region of hurricanes will extend. Due to this, Baatsen et al. (2014) showed that cyclones transformed from a hurricane can become more common especially in Western Europe and these storms can move northward. Global warming also reduces the temperature difference between polar regions and Equator and increases the altitude of the troposphere (Climate Nexus, 2015). These cause the jet stream to weaken, become more meandering and shift poleward, and the changes in the jet stream have been linked to cause more extreme weather events in Northern Hemisphere continents (Climate Nexus, 2015).

As stated in the previous paragraph, due to climate change more cyclones transformed from a hurricane can travel to Western Europe and move northward, and more extreme weather events can occur in Northern Hemisphere continents. Hence, an intense storm like Mauri to hit Finland more often in the future is possible. A major research challenge is therefore to investigate the impacts of climate change to the hurricane originated storms also in Finland. In order to do that, the indicators and

climatological conditions behind these storms have to be known as well as the capabilities and weaknesses in models illustrating them. Based on those, the weather alerting systems can be developed more reliable and accurate.

In this thesis, a hurricane originated storm and its background, structure evolution, synoptic features and climatic conditions were examined. By further researching these results and collecting a statistic examination of hurricane originated storms especially in Europe, the knowledge and understanding of these intense storms from hurricane background will be grown. That is essential for the development of storm warning systems and therefore for people to be safer and more prepared for the extreme weather in the future.

6. CONCLUSIONS

This master´s thesis investigated the evolution of hurricane Debby that transformed into storm Mauri in September 1982 using ERA-Interim reanalysis data produced by ECMWF. Hurricane Debby completed extratropical transition after passing Newfoundland, was caught up by westerlies and travelled rapidly across the North Atlantic while weakening. However, the transitioned cyclone ex-Debby located on the right side of jet entrance, which is a region of ascent and therefore enhances cyclogenesis, and did not decay. When reaching the UK, the structure of ex-Debby started to lose its asymmetricity and cold core features. There were positive pressure and temperature anomalies over central Europe making the jet stream, and ex-Debby following it, to shift north towards Scandinavia. The cyclone began to re-intensify and when crossing Sweden, ex-Debby had proceeded right ahead of an upper level trough which favours the cyclone development. That contributed a rapid deepening up to 27 hPa in 24 hours defining the storm as a meteorological bomb.

Another extratropical cyclone already existed across Europe resembling highly the Shapiro-Keyser cyclone model with perpendicular cold and warm fronts, the bent-back occluded front and a strong low pressure center. Ex-Debby interacted with the pre-

existing cold front, developed a strong low pressure center along the front and finally merged with the other low pressure center that was slowly weakening above the Norwegian Sea. Due to the occlusion and a forming warm seclusion of the other cyclone, which brought warmer air to the low pressure center of ex-Debby, the storm phased back to a warm cored system when crossing Sweden. When the cyclone reached Lapland and was named storm Mauri, the occluded bent-back front wrapped the storm tighter around it trapping warmer air inside the storm center and a warm seclusion formed. Due to that, the cyclone lost its frontal structure and became symmetric which is typical for an occlusion and barotropic environment. Hence, unlike an ordinary extratropical cyclone with cold cored and asymmetric structure, storm Mauri had a warm core and symmetric features. The strongest winds in Finland observed by Finnish Meteorological Institute (FMI) were 30 m/s so hurricane force wind speeds were just out of reach. Based on the ERA-Interim reanalysis, the strongest winds were only 17 m/s which is greatly underestimated compared to the observations from FMI.

Climatic conditions of September 1982 were examined and these features contributed the storm track to move northward. Central Europe was dominated by a strong high pressure area which caused a positive anomaly of mean sea level pressure, and the surface temperature anomaly was also strongly positive. These indicated anomalous anticyclonic circulation over that region leading to really weak winds. The jet stream was forced to take more northerly route as the high pressure area blocked its way towards east. Due to that, the storm tracks in general were driven towards higher latitudes. Also, positive NAO and AO phases favoured the storm track to shift northward. An extremely low activity hurricane season in 1982, with only two hurricanes, was influenced by a strong El Niño phase.

ERA-Interim reanalysis tracked the locations of the low pressure centers remarkably well when compared to NOAA but underestimated the surface pressure and wind speed values compared to FMI. In spite of that, ERA-Interim analysed the structure of the cyclone particularly well catching the whole extratropical transition process and evolution. Hence, ERA-Interim was found to be successful of tracking and calculating the cyclone evolution and characteristics.

ACKNOWLEDGEMENTS

I would like to thank my supervisor Hilppa Gregow and my superior Antti Mäkelä from the Finnish Meteorological Institute for introducing me to the fascinating topic for this thesis and for the useful comments along the way. Furthermore, I would like to thank my supervisor from the University of Helsinki, Victoria Sinclair, for having always time to help especially with the reanalysis issues. I thank ECMWF for providing the ERA-Interim reanalysis data, and for funding this thesis, I would like to thank the Finnish Meteorological Institute, the Suoma Loimaranta-Airila Fund, project ELASTINEN and project SAFIR-EXWE. Finally, I thank the people from Climate Service Centre unit for the much needed coffee breaks, and I would like to give my gratitude to my fellow students, friends and family for all the support and advice throughout the process.

REFERENCES

Ahrens, C. D., 2012. *Meteorology Today: An Introduction to Weather, Climate, and the Environment.* 10 ed. Belmont, USA: Cengage Learning.

Baatsen, M., Haarsma, R. J., Van Delden, A. J. & de Vries, H., 2014. Severe Autumn storms in future Western Europe with warmer Atlantic Ocean. *Clim. Dyn.,* Volume 45, pp. 949-964.

Bergens Tidende, 2006. *Bergen får 18 millioner for uvaerskader.* [Online]
Available at: http://www.bt.no/nyheter/lokalt/Bergen-far-18-millioner-for-uvarskader-1825782.html
[Accessed 30 3 2016].

Beven II, J. L. et al., 2008. Atlantic Hurricane Season of 2005. *Mon. Wea. Rev.,* Volume 136, pp. 1109-1173.

Bjerknes, J., 1919. On the structure of moving cyclones. *Geofys. Publ.,* Volume 1 (2), pp. 1-8.

Bjerknes, J. & Solberg, H., 1922. Life cycle of cyclones and the polar front theory of atmospheric circulation. *Geofys. Publ.,* Volume 3, pp. 3-18.

Browning, K. A., 2004. The sting at the end of the tail: Damaging winds associated with extratropical cyclones. *Q. J. R. Meteorol. Soc.,* Volume 130, pp. 375-399.

Böttger, H., Eckardt, M. & Katergiannakis, U., 1975. Forecasting extratropical storms with hurricane intensity unsing satellite information. *J. Appl. Meteor.,* Volume 14, pp. 1259-1265.

Clark, G. B., 1983. Atlantic Hurricane season of 1982. *Mon. Wea. Rev.,* Volume 111, pp. 1071-1079.

Climate Nexus, 2015. *The Jet Stream - A Science Backgrounder.* [Online]
Available at: http://climatenexus.org/learn/planetary-systems/jet-stream
[Accessed 30 3 2016].

Davis, C. A., Jones, S. C. & Riemer, M., 2007. Hurricane Vortex Dynamics during Atlantic Extratropical Transition. *J. Atmos. Sci.,* Volume 65, pp. 714-736.

Dee & NCAR Staff, 2016. *The Climate Data Guide: ERA-Interim.* [Online]
Available at: https://climatedataguide.ucar.edu/climate-data/era-interim
[Accessed 30 3 2016].

Dee, D. P. et al., 2011. The ERA-Interim reanalysis: configuration and performance of the data assimilation system. *Q. J. R. Meteorol. Soc.,* Volume 137, pp. 553-597.

Elsberry, R. L., 1995. *Global perspectives on tropical cyclones.* Geneva: World Meteor. Organization.

Evans, J. L. & Hart, R. E., 2003. Objective indicators of the life cycle evolution of extratropical transition for Atlantic tropical cyclones. *Mon. Wea. Rev.,* Volume 131, pp. 909-925.

Fink, A. H. et al., 2009. The European storm Kyrill in January 2007: synoptic evolution, meteorological impacts and some considerations with respect to climate change. *Nat. Hazards Earth Syst. Sci.,* Volume 9, pp. 405-423.

Frank, W. M., 1977. The structure and energetics of the tropical cyclone I: Storm structure. *Mon. Wea. Rev.,* Volume 105, pp. 1119-1135.

Goldenberg, S. B. & Shapiro, L. J., 1996. Physical Mechanisms for the Association of El Niño and West African Rainfall with Atlantic Major Hurricane Activity. *J. Climate,* Volume 9, pp. 1169-1187.

Grams, C. M. et al., 2011. The key role of diabatic processes in modifying the upper-tropospheric wave guide: a North Atlantic case-study. *Q. J. R. Meteorol. Soc.,* Volume 137, pp. 2174-2193.

Gray, W. M., 1984. Atlantic Seasonal Hurricane Frequency. Part I: El Niño and 30 mb Quasi-Biennial Oscillation Influences. *Mon. Wea. Rev.,* Volume 112, pp. 1649-1668.

Haarsma, R. J. et al., 2013. More hurricanes to hit western Europe due to global warming. *Geophysical Research Letters,* Volume 40, pp. 1783-1788.

Hart, R. E., 2003. A cyclone phase space derived from thermal wind and thermal asymmetry. *Mon. Wea. Rev.,* Volume 131, pp. 585-616.

Hart, R. E. & Evans, J. L., 2001. A Climatology of the Extratropical Transition of Atlantic Tropical Cyclones. *J. Climate,* Volume 14, pp. 546-564.

Hodges, K. I., Lee, R. W. & Bengtsson, L., 2011. A Comparison of Extratropical Cyclones in Recent Reanalyses ERA-Interim, NASA MERRA, NCEP CFSR, and JRA-25. *J. Climate,* Volume 24, pp. 4888-4906.

Holton, J. R. & Hakim, G. J., 2013. *An Introduction to Dynamic Meteorology.* 5th ed. The United States: Academic Press.

Hoskins, B. J., McIntyre, M. E. & Robertson, A. W., 1985. On the use and significance of isentropic potential vorticity maps. *Q. J. R. Meteorol. Soc.,* Volume 111, pp. 877-946.

Jarvinen, B. R., Neumann, C. J. & Davis, M. A. S., 1984. A tropical cyclone data tape for the North Atlantic basein, 1886-1983: Contents, limitations and uses. *NOAA Tech. Memo. NWS NHC-22,* p. 21 pp..

Jones, S. C. et al., 2003. The Extratropical Transition of Tropical Cyclones: Forecast Challenges, Current Understanding, and Future Directions. *Weather and Forecasting,* Volume 18, pp. 1052-1092.

Klein, P. M., Harr, P. A. & Elsberry, R. L., 2000. Extratropical transition of western North Pacific tropical cyclones: An overview and conceptual model of the transformation stage. *Weather and Forecasting,* Volume 15, pp. 373-396.

Knapp, K. R. et al., 2010. The international best track archive for climate stewardship (IBTrACS): Unifying tropical cyclone best track data. *Bulletin of the American Meteorological Society,* Volume 91, pp. 363-376.

Kocin, P. J. & Uccellini, L. W., 1987. The Interaction of Jet Streak Circulations during Heavy Snow Events along the East Coast of the United States. *Wea. Forecasting,* Volume 2, pp. 289-308.

Lackmann, G., 2012. *Midlatitude Synoptic Meteorology: Dynamics, Analysis, and Forecasting.* Boston, USA: Amer. Meteor. Soc..

Lin, Y.-L., 2007. *Mesoscale Dynamics.* Cambridge: Cambridge University Press.

Malmquist, D., 1999. Meteorologists and insurers explore extratropical transition of tropical cyclones. *Eos, Trans. Amer. Geophys. Union,* Volume 80, pp. 79-80.

Marshall, J. & Plumb, R. A., 2007. *Atmosphere, Ocean and Climate Dynamics.* Cambridge, USA: Academic Press.

Merrill, R. T., 1993. *Tropical cyclone structure - Chapter 2.* Geneva: Global Guide to Tropical Cyclone Forecasting, WMO/TC-No. 560, Report No. TCP-31, World Meteorological Organization.

Miller, B. I., 1985. On the maximum intensity of hurricanes. *J. Meteor.,* Volume 15, pp. 184-195.

NCAR Analyzed and Model Data, 2016. *An Introduction to Atmospheric and Oceanographic Datasets.* [Online]
Available at: http://www.cgd.ucar.edu/cas/tn404/text/tn404_9.html
[Accessed 30 3 2016].

NOAA Data Registry, 2014. *Digital Coast.* [Online]
Available at: https://coast.noaa.gov/dataregistry/search/collection/info/hurricanes
[Accessed 18 1 2016].

NOAA Historical Hurricane Tracks, 2016. *Hurricanes - The Improved Historical Hurricane Tracks Tool.* [Online]
Available at: coast.noaa.gov/hurricanes/
[Accessed 22 2 2016].

NOAA Monitoring & Data: Index Values, 2015. *Climate Prediction Center - Monitoring & Data: Current Monthly Atmospheric And Sea Surface Temperatures Index Values.* [Online]
Available at: http://www.cpc.ncep.noaa.gov/data/indices/
[Accessed 9 11 2015].

NOAA News, 2014. *Slow Atlantic hurricane season coming to a close.* [Online]
Available at:
http://www.noaanews.noaa.gov/stories2013/20131125_endofhurricaneseason.html
[Accessed 9 11 2015].

NOAA Teleconnection Index Calculations, 2015. *Climate Prediction Center - Teleconnection Index Calculations.* [Online]
Available at: http://www.cpc.ncep.noaa.gov/data/teledoc/teleindcalc.shtml
[Accessed 9 11 2015].

NOAA Teleconnection Pattern Calculation Procedures, 2015. *Climate Prediction Center: Teleconnection Pattern Calculation Procedures.* [Online]
Available at:
http://www.cpc.ncep.noaa.gov/products/precip/CWlink/daily_ao_index/history/method.shtml
[Accessed 9 11 2015].

NOAA Warm Episodes, 2012. *Climate Prediction Center - Warm Episodes.* [Online]
Available at:
http://www.cpc.ncep.noaa.gov/products/analysis_monitoring/impacts/warm_impacts.shtml
[Accessed 18 2 2016].

Palmén, E., 1948. On the formation and structure of tropical hurricanes. *Geophysica,* Volume 3, pp. 26-38.

Powell, M. D., 1982. The transition of the Hurricane Frederic boundary-layer wind fields from the open Gulf of Mexico to landfall. *Mon. Wea. Rev.,* Volume 110, pp. 1912-1932.

Sanders, F. & Gyakum, J. R., 1980. Synoptic-Dynamic Climatology of the "Bomb". *Mon. Wea. Rev.,* Volume 108, pp. 1589-1606.

Schott, T. et al., 2012. *The Saffir-Simpson Hurricane Wind Scale,* s.l.: NOAA.

Schultz, D. M., Keyser, D. & Bosart, L. F., 1998. The effect of large-scale flow on low-level frontal structure and evolution in midlatitude cyclones. *Mon. Wea. Rev.,* Volume 126, pp. 1767-1791.

Shapiro, M. A. & Keyser, D., 1990. Fronts, jet streams and the tropopause. *Extratropical Cyclones, The Erik Palmén Memorial Volume, C. W. Newton and E. O. Holopainen, Eds., Amer. Meteor. Soc.,* pp. 167-191.

Swiss Re Group, 2008. *New Swiss Re sigma study: Catastrophe losses in 2007 were highest in Europe.* [Online]
Available at:
http://www.swissre.com/media/news_releases/Catastrophe_losses_in_2007_were_highest_in_Europe.html
[Accessed 30 3 2016].

Thompson, D. W. J. & Wallace, J. M., 1998. The Arctic Oscillation signature in the wintertime geopotential height and temperature fields. *Geophys. Res. Lett.,* Volume 25, pp. 1297-1300.

Uccellini, L. W., 1990. Processes contributing to the rapid development of extratropical cyclones.Palmen Memorial Symposium on Extratropical Cyclones. *Amer. Meteor. Soc.,* pp. 289-308.

Walker, G. T., 1924. Correlation in seasonal variation of weather. IX. A further study of world weather. *Mem. Ind. Meteor. Dept.,* Volume 24, pp. 275-333.

Wallace, J. M. & Hobbs, P. V., 2006. *Atmospheric Science: An Introductory Survey - 8.1.5. In Search of the Perfect Storm.* 2nd ed. Burlington, USA: Academic Press.

Vallis, G. K. & Gerber, E. P., 2008. Local and hemispheric dynamics of the North Atlantic Oscillation, annular patterns and the zonal index. *Dyn. Atmos. Oceans,* Volume 44, pp. 184-212.

Woollings, T., Hannachi, A. & Hoskins, B., 2010. Variability of the Nort Atlantic eddy-driven jet stream. *Q. J. R. Meteorol. Soc.,* Volume 136, pp. 856-868.